RSC Advances

REVIEW

View Article Online
View Journal | View Issue

Cite this: *RSC Adv.*, 2026, **16**, 13040

A review on multifunctional applications of MgO nanostructures: from material science to environmental and agricultural innovations

G. Georgelin Jeba Mahiba, A. Prabakaran * and Babu Balraj

Green synthesis of magnesium oxide nanoparticles (MgO NPs) using plant extracts and bio-waste materials represents a sustainable alternative to conventional synthesis methods. MgO, characterized by its crystalline lattice of Mg^{2+} and O^{2-} ions, exhibits hygroscopic properties and is a white, solid mineral with diverse technological applications. These nanoparticles demonstrate versatile applications across multiple disciplines, including agriculture, drug delivery, environmental remediation, antimicrobial treatments, and supercapacitor technologies. Previous studies describe diverse synthesis methodologies including sol–gel routes, flame synthesis, and hydrothermal methods, whereas this review focuses primarily on green synthesis approaches. The green synthesis methodology employs plant extracts that serve dual functions as both reducing agents and capping agents in the formation and stabilization of metal oxide nanoparticles. Biosynthesized MgO NPs exhibit distinctive properties, including controlled morphology, high surface area, tunable particle size distribution, and enhanced stabilization. These characteristics position MgO NPs as promising candidates for addressing contemporary environmental challenges and advancing energy storage technologies. This review critically analyzes recent developments in biosynthesized MgO NPs, highlighting the advantages of green synthesis over conventional methods and identifying key research gaps and future directions in this rapidly evolving field.

Received 16th September 2025
Accepted 9th February 2026

DOI: 10.1039/d5ra07016c

rsc.li/rsc-advances

1 Introduction

Nanotechnology and nanostructured materials are the fastest-growing areas of the 21st century. They have many uses in medicine, energy storage, material science, the environment, information technology, and biotechnology. The basic idea behind the increased interest is that materials can exhibit properties at the nanoscale that are not possible at the micro- and macroscales.[1] Most people agree that nanoparticles are materials that are no bigger than 100 nm.[2] These nanoparticles are used in a variety of industries, including coatings, petrochemical goods, electronics, fiberboards, metallic ceramics, and catalysis. Because of their enormous surface-to-volume ratio, high atom count, and compact size, nanostructures are considered unusual materials. Dimensionality (0D–3D), morphology (nanosphere, nanofilm, nanotube, nanobelt, nanorod, nanowire), state (isometric, suspension, agglomerates), and chemical composition (organic, inorganic, single component, composites) are the four ways in which nanomaterials can be classified.[3–5] There are some samples with sizes ranging from 0D to 3D and with different shapes.[6] In the first scenario, organic-based nanostructures such as ferritin, liposomes, micelles, and dendrimers are highly environmentally friendly and effective for drug delivery.[7] Metal-based and metal-oxide-based materials are two more types of inorganic materials.[8] Metal-based nanomaterials are made from metals such as Au, Cu, Se, and Ag.[9] Cosmetics, chemicals, food manufacturing companies, gene transfer, and thermal ablation are just a few of the industries in which they are employed.[10] Large bandgaps, low dielectric constants, low refractive indices, good chemical stability, and the existence of unoccupied oxygen sites are among the distinctive characteristics of metal oxide nanoparticles. Because of their many uses, MgO NPs are particularly interesting due to their abundance, nontoxicity, affordability, odorlessness, stability, magnetization, crystallinity, absorptivity, electrical and thermal conductivity, stoichiometry, high surface area, and reactivity. Because of these incredible qualities, MgO nanoparticles are now at the forefront of nanomedical research.[11,12] Magnesium oxide (MgO), ferric oxide (FeO), zinc oxide (ZnO), titanium dioxide (TiO_2), copper oxide (CuO), silver oxide (Ag_2O), and nickel oxide (NiO) are the most well-known members of the single metal oxide group. When a metal and oxygen mix to form an oxide, metal oxide-based compounds are produced.[13–15] The new green nanotechnology approach employs a number of techniques to protect the earth's crust by eliminating or lowering dangerous chemical levels.[16] The extracts contain significant amounts of carbon, hydrogen, and nitrogen, as well as phytochemicals such as flavonoids, alkaloids, and phenolics. The plant extract and metal salts combine to create nanoparticles with varying sizes, shapes, and surface areas.

Department of Physics, Vel Tech Rangarajan Dr Sagunthala R&D Institute of Science and Technology, Avadi, Chennai-600 062, Tamil Nadu, India. E-mail: draprabakaran@veltech.edu.in

Due to the enormous demand for the raw material, there has been a push to identify new uses for NPs utilizing a green synthesis approach[17] from microorganisms such as yeast, algae, fungi, and bacteria.[18] Another thing that makes the property distinctive is that the extract of leaves breaks down faster than biological sources. NPs can be produced using a variety of chemical synthesis techniques, including the sol–gel process, simple combustion, laser vaporization, aerosol synthesis, chemical gas-phase deposition, micelle-mediated synthesis, flame pyrolysis, the hydrothermal route, aqueous wet-chemical precipitation, surfactant approaches, and more. The ecosystem and ecology are under threat due to the toxic chemicals used to produce nanoparticles, which also have detrimental effects on individuals. Once MgO particles are extremely small, such as nanoparticles, it is possible to experimentally determine their primary characteristics, including their poor electrical conductivity, strong thermal stability[19–22] and catalytic activity. MgO, commonly known as periclase,[23] is an inorganic material with a molecular mass of 40.31 g mol^{-1}[24] and a density of 3.58 g cm^{-3}. Its lattice is composed of Mg^{2+} and O_2 ions joined by an electrovalent connection or ionic bond in a $1s^2$ $2s^2$ $2p^2$ configuration, indicating that the d orbitals are unoccupied.[25] Magnesium oxide's structure resembles that of rock salt (lattice parameter 4.21 Å).[26] It is typically composed of two Mg and O lattices that are offset by half of the body diagonals and cross one another[27] and the complete overview is represented in Fig. 1.

There have been many research studies over the last 10 years on how to make MgO NPs in a green way. So, it was prime to write a review article that summarizes the most recent developments in MgO NPs (Fig. 1). We analyze the structure, morphology, and manufacturing processes of MgO nanostructures derived from various sources, including orange fruit peel, papaya leaf extract, neem leaves, *Trigonella foenum graecum* (fenugreek), spinach plant extract, and mushroom extract.[28] We have focused on the most recent developments and uses of these nanomaterials. The problems and future prospects include difficulties reproducing results and controlling particle size and shape. There is also a lack of conceptions of the mechanisms, particularly in biological synthesis, and protocols need to be standardized and improved. It discussed (i) an updated overview of synthesis methods (ii) discussion of their structural and physicochemical characteristics; (iii) their multifunctional applications in fields related to energy, agriculture, biomedicine, and the environment; and (iv) a summary of current limitations and future research control aimed at enhancing mechanistic understanding, reproducibility, and scalability.[29,30]

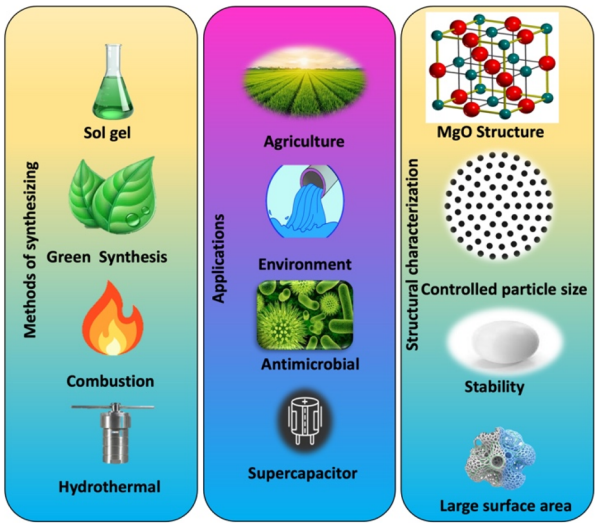

Fig. 1 Synthesis methods, structural features, and applications of MgO.

2 Various methods of preparing MgO NPs

2.1 High energy ball milling (HEBM) technique for large-scale nanomaterial synthesis

A simple method for generating materials in large quantities is high-energy ball milling (HEBM), also known as mechanical grinding, mechanical milling, or mechanical alloying. This process has generated particles with diameters from 4 to 26 nm. Usually, chemical reactions that modify reactivity occur in this process, but this approach, however, has run into several issues, including contamination from the surrounding atmosphere or milling. Given its extensive use, including in hip implants and bone screws, we can tailor the manufacturer of the fine powder to bulk form. Among the various benefits this HEBM offers are its low cost and the ease with which the operation can be scaled to generate vast amounts of material. Nitrides are produced during milling from the oxygen or nitrogen present.

Typical elements influence the synthesis process is milling time. Finer particle sizes are usually achieved with longer grinding durations. Higher rotational speeds are necessary to enhance impact force and can also result in smaller particle sizes. The smaller, more numerous balls can improve the grinding process but also increase the risk of contamination from the balls themselves. Higher ball-to-material ratios usually result in faster grinding but can also lower overall efficiency. The size and shape of the container can affect how the grinding medium is distributed and how it works. HEBM method is shown in Fig. 2(a–c).[31,32]

There are two mechanisms used in the ball milling process (i) impact and attrition and (ii) size reduction. In the grinding media, represent Fig. 2(a) overall milling process, Fig. 2(b) breaking phase, Fig. 2(c) welding phase, balls collide with the material as they rotate within the container, generating localized high pressures and influencing force. The material's surface and edges are worn away by the constant friction and contact with the balls, thereby reducing its size. In size reduction, the combination of impact and attrition forces the material to fracture and break down into very small pieces. The milling process can reduce the particle size to nanoscale dimensions, making it suitable for synthesizing nanomaterials.

2.2 High-throughput synthesis of MgO NPs by flame spray pyrolysis technique

It is used for one of the rapid methods for preparing magnesium oxide nanoparticles. This technique involved dissolving

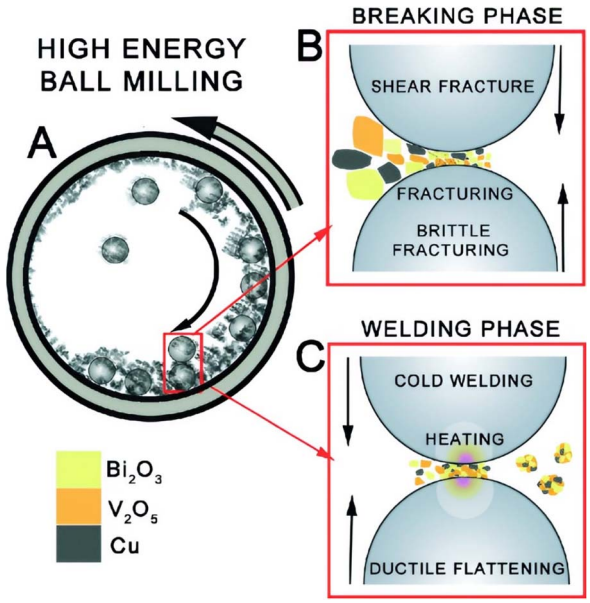

Fig. 2 Shows the process by which high-energy ball milling produces mechanical alloying and nanocomposite materials: (a) overall milling process, (b) breaking phase, (c) welding phase. Reproduced under terms of the CC-BY license. Copyright 2017, Victor-ishrayelu Merupo, published by *CrystEngComm3*.[33]

an appropriate amount of distilled water and mixing a 1 M (1 Molar) hexamethylenetetramine solution with a 1 M magnesium nitrate solution while stirring continuously for 10 minutes at room temperature) (Fig. 3(a)). We next poured the ready solution into a spray pyrolysis chamber (Fig. 3(b)). The reaction unit was constructed from a capillary tube with an opening diameter of 1.2 mm and an exterior diameter of approximately 1 mm (internal diameter of approximately 0.6 mm). It was a flame-spray device with a fine nozzle assisted by high-pressure gas. The spray dispersed(gFig. 3(b)) and was supported by flamelets. A SiO_2 substrate collected the product; a flow controller regulated the solution dispersion flow rate. Fig. 3 represents the synthesis of MgO NPs by the FSP method.[34–39]

Three different kinds of atomizers are available and each is described ultrasonic wave nebulizer: used to generate mists from liquids and produce sprays using high-frequency vibrations. A small particle is produced when the fog enters the flame by following the vapor for aerosol flame synthesis (VAFS) path. Atomizing gas facilitates the separation of liquid into a spray, which is accomplished by two-fluid nozzles. An electro sprayer uses high voltage to turn liquid into an aerosol. It facilitates the production of ions from macromolecules. Two-fluid nozzles are the most frequently utilized atomizers for FSP systems. The purpose of burners is to produce a flame. Diffusion burners and premixed burners are two different types of burners. The fuel and oxidant were blended by the premixed burner.[41] The burner system is ignited by the self-sustaining flame produced by FSP. By altering the precursor's metal concentration and combustion enthalpy, it has the advantage of directly controlling particle size.[42,43] The collector's job is to collect the FSP operation's output. Particle collection is typically carried out on a filter or substrate.

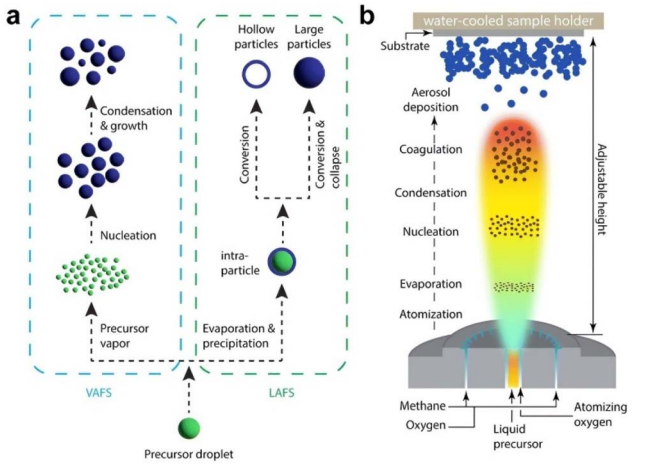

Fig. 3 Shows two crucial elements of producing nanoparticles utilizing flame spray techniques: (a) particle formation mechanism,(b) flame spray pyrolysis. Reproduced with permission from ref. 40. Copyright 2017, *Nanoscale*.

2.3 Hydrothermal synthesis route for MgO

In this synthesis method, magnesium nitrate hexahydrate ($Mg(NO_3)_2 \cdot 6H_2O$) and sodium hydroxide (NaOH) were the precursor materials, while cetyl trimethyl ammonium bromide (CTAB) was the surfactant. Add the magnesium nitrate solution dropwise to the sodium hydroxide solution. The pH of the solution was measured after adding NaOH; it was almost 10.2 (alkaline), and it swirled continuously for 60 minutes. After a white precipitate formed, it was transferred to a Teflon-jar and heated to a steady temperature for hydrothermal treatment. To remove any ionic contaminants, the white precipitate was also filtered, dried overnight in a hot-air oven, then cleaned with ethanol and water. The dry powder was then transferred to a silica crucible, where it was reduced in a muffle furnace. A mortar and pestle were used to properly grind the resultant material into powder after it had cooled. Fig. 4 shows the hydrothermal synthesis of MgO NPs. The benefits of HT synthesis are that it is a very straightforward process that can be scaled up. We can then produce nanoparticles with the required characteristics by controlling particle size and shape. Generally speaking, it is regarded as an environmentally advantageous procedure.[44,45]

Magnesium hydroxide precursors spontaneously nucleate and expand uncontrollably during the hydrothermal synthesis of MgO nanoparticles in the absence of CTAB mediation. Unevenly shaped and polydisperse nanoparticles arise because there is no stabilizing ingredient to stop particle agglomeration in the absence of the surfactant. Because it lowers surface energy and functions as a soft template, CTAB, a cationic surfactant, is essential for regulating the size, shape, and surface properties of MgO particles.[47,48] It makes it easier for evenly spaced, nanoscale MgO particles with increased porosity and surface area to form. On the other hand, the non-CTAB-assisted approach often results in lower surface activity, poor dispersion, and larger crystallite sizes. Therefore, compared to those synthesized without surfactant aid, the CTAB-mediated

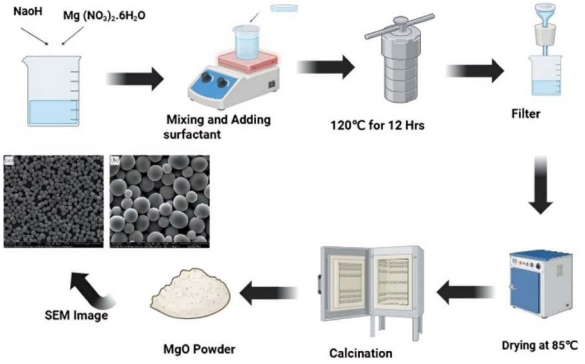

Fig. 4 Depicts the hydrothermal methodical synthesis of MgO NPs (Xiaoyun Song, published by Research Gate Inserted SEM[46]).

hydrothermal approach offers a clear benefit by producing highly crystalline, morphologically uniform MgO nanoparticles that exhibit improved catalytic, optical, and antibacterial activity.[30] The establishment of this comparison underscores the importance of surfactant-mediated control in tailoring the physicochemical properties of MgO nanostructures for specific applications. Sodium dodecyl sulphate (SDS)[49,50] polyvinylpyrrolidone (PVP),[51] Triton X-100, and Tween 80 are other frequently utilized surfactants for the creation of MgO NPs.[52] Since the ideal surfactant selection for MgO nanoparticle synthesis relies on the desired application and the particular attribute being targeted, such as size, morphology, surface area, or functionality, there is no one best surfactant that works for all situations. When creating highly crystalline, homogeneous, and evenly distributed magnesium oxide nanoparticles with a large surface area and improved physicochemical properties, CTAB is often preferred among surfactants. Studies further show that while other surfactants, such as PVP, Triton X-100 (nonionic), and SDS (anionic), can stabilize particles and affect nanoparticle shape, CTAB often provides superior control over particle size and dispersion, particularly for catalysis or antibacterial applications. Although amphoteric or mixed surfactant systems may occasionally perform better for specific functions, CTAB remains the industry standard for the manufacture of high-quality MgO nanoparticles.[53,54] Each of these surfactants has a unique effect on particle size, shape, and dispersion. Before starting the hydrothermal or sol–gel process, dissolve the selected surfactant in the reaction mixture with the metal precursors. The surfactant molecules will function as templates or stabilizers, regulating nucleation and growth to produce nanoparticles with the required properties. Depending on the intended use and target morphology, the surfactant type and concentration should be tuned.[55,56]

The wet chemical method, hydrothermal method, co-precipitation method, sol–gel method, microwave-assisted method, and template-assisted method are some of the several synthesis techniques. The sol–gel technique is widely regarded as the most suitable and widely used technology for the production of MgO NPs. The green techniques depicted in Fig. 5 are demonstrated to lower the risk of harm to humans and the environment by prioritizing nontoxic, bio-safe substances. This methodology has several distinct advantages over other conventional methods. The sol–gel method, which yields incredibly clean and homogeneous nanoparticles, enables molecular-level precursor mixing. It makes it easy to manage particle size, between 10 and 50 nm, and form by exactly regulating important reaction parameters like pH, temperature, and calcination time. Another advantage is that it uses less energy and equipment than hydrothermal or solid-state processes because it works at comparatively modest synthesis temperatures. This method yields MgO NPs with exceptional crystallinity and a high specific surface area, which makes them perfect for catalytic, adsorption, and antibacterial uses. Laboratory-scale synthesis and industrial production. Therefore, this method continues to be the most effective means to create MgO nanoparticles of exceptional quality with unique structural and functional properties.

Because even little variations can alter the size and structure of the particles, the sol–gel method for creating MgO NPs has the disadvantage of requiring extremely exact control over pH, temperature, and humidity. Long reaction durations are another drawback of this approach, and if stabilizers or surfactants are not included, agglomerated nanoparticles may result. Furthermore, it is challenging to scale up the process for industrial manufacturing because some of the precursors and solvents utilized are expensive or dangerous. In a similar vein, the co-precipitation technique for creating MgO nanoparticles has a number of drawbacks.[57,58] It often necessitates high-temperature post-calcination, which can lead to non-uniform particle sizes, particle growth, and a reduction in surface area. Because variations in pH and reaction rate might result in the development of pollutants, precise control is crucial, so this method[59] is not always able to produce complex-doped nanoparticles. The hydrothermal method of creating MgO NPs has the disadvantage of needing high-pressure, high-temperature equipment, and the reactions frequently take a long time to finish. The energy-intensive nature of the process and the challenge of regulating particle aggregation make large-scale production impractical, and some of the solvents utilized in this process might be dangerous.[60] Producing MgO NPs by burning or combustion has a number of disadvantages. Even though inhomogeneous heating may produce heterogeneous particle sizes, the high temperatures involved may cause particle sintering and a loss of nanoscale characteristics. Controlling the form and porosity of nanoparticles can

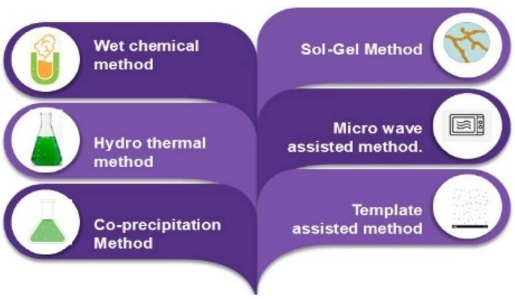

Fig. 5 Shows the different synthesis methods.

frequently be challenging, and some of the precursors utilized in this process may be hazardous or explosive. Using a microwave-assisted method to produce MgO NPs has a number of drawbacks. Rapid heating can result in non-uniform nucleation, which can lead to variances in particle size, and the equipment needed is more costly than with traditional heating methods. This approach is usually limited to small-scale synthesis unless specialized industrial microwave reactors are used. Reaction parameters need to be carefully adjusted in order to obtain correct results.[58]

Long processing times are required for the sol–gel method to produce MgO NPs, especially during the gel formation and drying phases that follow. Furthermore, the overall manufacturing cost is frequently increased by the use of expensive chemical solvents and precursors. Moreover, the sol–gel technique is less practical for large-scale manufacturing due to the considerable difficulties involved in scaling it up to industrial levels.[61,62] The ecologically friendly production of magnesium oxide nanoparticles using plant extracts is constrained by a number of reasons. First, differences in plant extract content may lead to anomalies and compromise the uniformity of nanoparticle synthesis. The extracts of complex macromolecules may complicate the purification procedure. Additionally, green synthesis methods provide less control over the particle size distribution than physical synthesis approaches.[63,64] There are several restrictions on the synthesis of MgO NPs by combustion, which uses high temperatures that can cause particle agglomeration, reduce the uniformity and homogeneity of the NPs and make it challenging to control particle morphology. To maintain environmental compliance and safety, the process also produces gaseous waste that requires adequate ventilation.[65] High-pressure reactors, which are expensive and increase the total equipment investment, are necessary for the HT method of generating MgO nanoparticles. Long reaction times are often required for this approach to yield the desired NP characteristics. Furthermore, batch sizes may be restricted by equipment constraints, making scale-up difficult for industrial applications.

3 Green synthesis strategies: economic and environmental benefits in nanotechnology

Green synthesis helps to reduce the carbon footprint. Reducing synthetic steps and reducing waste generation from green methods helps to lower demand for costly garbage disposal or remedial measures. Plant-mediated synthesis, for example, may be more cost-effective than conventional methods, as plant extracts are easily obtained and available.[66] Reduced trash generation translates into reduced waste disposal and associated remedial expenditures. Green synthesis enables plant extracts or biomolecules to be used to control the size, form, and composition of nanoparticles. Due to their versatility, green technologies can yield traits suitable for numerous applications, including environmental cleanup, biotechnology, and medicine, thereby benefiting diverse sectors. Some green methods can produce faster reaction rates and better yields, therefore increase production and reduce the demand for expensive reagents. A comparative table on green synthesized MgO has been given in Table 1.

Green synthesis enables plant extracts or biomolecules to regulate the size, form, and composition of nanoparticles. The adaptability of green techniques allows the production of nanoparticles with specialized properties suitable for various applications, including environmental cleanup, biotechnology, and medicine. Additional benefits include the fact that certain environmentally friendly methods can increase yields and reaction rates, increase output, and reduce the need for expensive chemicals. Green techniques minimize the risk of injury to people and the environment by prioritizing nontoxic, biodegradable chemicals. Using microorganisms as Fungai, Bacteria, and Algae, the green method (GM) achieves the synthesis of MgO NPs. Orange fruit, mushroom extract, neem leaves, spinach, watermelon fruit, jamun fruit, papaya, aloe vera leaves, lemon, apple peels, wood apple, rosemary, *Phyllanthus embolica* fruit, and so forth are among the plant extracts. A general green synthesis method is shown in Fig. 6.

Making MgO NPs from orange fruit waste involves three fundamental steps: (i) making an extract from orange peels; (ii) making a solution of magnesium nitrate; and (iii) making MgO NPs in an eco-friendly way. Orange fruit peel was collected and allowed to air dry before being ground into a powder. A 250 ml beaker was filled with 100 ml of filtered water and 10 g of orange peel powder. Stirring continually for an hour was the treatment. Whatman filter paper was used to filter the extract. Peel extract was added to the magnesium nitrate solution after 5 g of magnesium nitrate and 100 ml of deionized water were combined. Then, drop by drop, the sodium carbonate solution was added. A change in hue indicated that the magnesium nitrate solution had been converted to magnesium oxide using a magnetic stirrer. After that, stirring continued for four hours. A carbonate solution will be used to maintain the combination's pH at 12. During this time, nanoparticles form and settle near the bottom of the flask. Next, centrifuge at 5000 rpm min^{-1} for 5 minutes. After filtering, the nanoparticles were left to air-dry overnight.

Magnesium nitrate serves as the precursor for the formation of MgO, while neem (*Azadirachta indica*) leaf extract serves as the reducing agent. Five grams of fresh neem leaves should be repeatedly rinsed with ordinary water and then distilled water before being dried for 15 to 20 minutes at 60°. Freshly made neem leaf extract was used to create MgO NPs. For the experiment, 5 ml of leaf extract and 20 ml of distilled water were added to a 250 ml beaker, which was then heated to 60 °C. The liquid is heated to 80 °C for four hours while being constantly stirred after adding five grams of magnesium nitrate. Neem leaf extract was used to transform the $Mg(NO_3)_2$ ions into magnesia or MgO nanoparticles. When MgO NPs start to develop, the color of the solution shifts from yellow to yellowish–brown.[85–87]

This method uses magnesium sulphate to create MgO nanoparticles. First, collect the fresh leaves of the mango, papaya, and neem. After being cleaned with regular water, the leaves of papaya (Pa), neem (Ne), and mango (Ma) were rinsed

Table 1 Comparative analysis of MgO's performance with other relevant studies

S. No.	Calcinating temperature	Synthesizing method	Precursor material	Morphology	Calcinating time	Particle size	Route of synthesis	Applications	Ref.
1	400	Green (biogenic) wet chemical precipitation method	Magnesium nitrate	Product is agglomerated and particle in nature	4 h	—	Plant-neem	Green emission occurs at 550 nm, blue emission occurs at 470 nm, and violet emission occurs at 390 nm photocatalytic activity for methylene blue (MB) dye degradation when exposed to UV and solar light	67
2	—	Green method	Magnesium nitrate	Rod-like morphology with needle-shaped edges	—	—	Neam leaf	Gram-negative bacteria (*Salmonella typhimurium*, *Enterobacter aerogenes*) and Gram-positive bacteria (*Enterococcus faecalis*, *Bacillus subtilis*, *Enterococcus*)	68
3	500 °C	Plant mediated green synthesis	Magnesium nitrate	Spherical to aggregated nanoparticles	4 h	Size 231.1 nm	Neem leaf	Seed germination process using *Cicer arietinum* (chick pea) and *Solanumlycopersicum* (tomato)	69
4	—	Plant-mediated green synthesis	Magnesium nitrate	Spherical shell shape	90 min	90–100 nm	Neem	The highest level of decolorization (91%) was achieved using reactive red 195 dye at a concentration of 0.02% and a catalyst quantity of 0.003 g L^{-1}	70
5	—	Green synthesis	Magnesium nitrate	—	4 h	—	Neem (Azadirachta indica leaves	Methylene blue solution, DPPH test, and 88% dye degradation demonstrated strong ($P < 0.0001$) antioxidant capabilities with 80% DPPH scavenging activity at 100 mg ml^{-1} concentration	71
6	500 °C	Green solution combustion	Magnesium sulfate	Irregular shaped particles, and a thin irregular flake-like structure	2 h	—	Mango, neem, papaya	In opposition to human pathogens such *Pseudomonas aeruginosa*, *Staphylococcus aureus*, and *Escherichia coli*	29
7	600 °C	Green chemistry	Magnesium nitrate	Iirregular agglomerated nanoparticles	4h	168.7 nm from banana peel and 206.4 nm	Bark	Photocatalytic, antioxidant, antibacterial, and cytotoxicity activities	72
8	Green synthesis	Magnesium nitrate	Clearly sphere-shaped, uniform, and in aggregated form				Leaf	81% Photocatalytic degradation of rhodamine MB dye antibacterial potential against the bacterial strains of *E. coli* and *R. solanacearum*	73
9	400 °C	Bio-combustion method	Magnesium nitrate	Sponge structure with porous	—	100–200	Fruit extract	90% Evans blue dye degradation	74
10	400	Plant-based green synthesis	Magnesium nitrate	Spherical and agglomerated	2	200 nm	Green tea	88% degradation of Victoria blue dye	75
11		Solution combustion synthesis	Magnesium nitrate	Quasi spherical shapes	24	—	Cinnamon bark extract	95% photocatalytic degradation of methyl orange dye	76
12		Green approach	Magnesium nitrate	quasiSpherical shaped	6	32.6 nm	Fruit	Photocatalytic removal of rhodamine B and methylene blue dyes	77
13	873 °C		Magnesium nitrate		—	52–68	Algae extract		78

Table 1 (*Contd.*)

S. No.	Calcinating temperature	Synthesizing method	Precursor material	Morphology	Calcinating time	Particle size	Route of synthesis	Applications	Ref.
		Co-precipitation method		Flake-like morphology				95% photocatalytic degradation of rhodamine B and methylene blue dyes	
14	60 °C oven	Green synthesis	Magnesium nitrate	Spherical shaped	—	—	Plant	95.8% reactive brown 9 dye breakdown using photocatalysis	79
15	500 °C	Bio synthesis	Magnesium nitrate	Aggregated form	4 h	~65	Leaf	83.47% degradation of direct red-31 and 65.52% for reactive golden yellow-145	80
16	550 °C	Co-precipitation method	Magnesium nitrate	Aggregated, spherical or hexagonal morphology	6 h	20–50	Bark, leaf, flower	99.7% degradation and elimination of congo red and crystal violet, two organic colors	81 and 89
17	500 °C	Biosynthesis	Magnesium nitrate	Flower shaped	3 h	68.02	Algae	Anticancer, antimicrobial and photocatalytic activities,cytotoxic activity against lung cancer cell lines A549	82
18	400 °C	Bio synthesis	Magnesium nitrate	Rod, rectangular-shaped	3 h	~85, 18.6–27.6	Fungal	92.8% photocatalytic degradation of real textile effluent, antimicrobial activity against Gram-positive, Gram-negative, and unicellular fungi	83

with distilled water and 1% sodium hypochlorite to remove any remaining dirt. They were allowed to air-dry for 8 days before being ground into a powder in a mortar and pestle. For eight hours, the shaker incubator was operated at 130 rpm while 10 g of leaf powder and 100 ml of distilled water were combined. The fluid was initially filtered, and then nanoparticles were subsequently made from the filtrate. 50 ml of filtrate was mixed with 3 mg of Mg SO_4 that had been heated to 100 °C for 30 minutes. The growth of nanoparticles was shown by colour changes from green to brown. Following evaporation, the black solid was calcined at 500 °C to aid in morphological and structural analysis, as shown in Fig. 7.[68,88–91]

Twenty-five grams of fresh button mushrooms were gathered and repeatedly cleansed with distilled water and running tap water to remove any organic pollutants. They were then divided into small pieces and added to a 2.2-liter beaker containing 250 ml of distilled water. For half an hour, the beaker was continuously and thoroughly stirred with a magnetic stirrer. The extract is then filtered with Whatman filter paper. In this instance, the synthesis of MgO NPs is stabilized and decreased by the mushroom extract. An aqueous solution containing 0.1 M of magnesium acetate solution at 40 °C was used to swirl the mushroom extract for two hours continuously Fig. 8. The giant changes from colourless to light brown in less than half an hour when magnesium acetate is present. The mixture is then heated on a plate to complete the combustion. The final products were calcined at 400 °C for 4 hours to produce MgO NPs.[92,93]

After being cleaned with distilled water and allowed to air dry, aloe vera leaves, fresh watermelon (*Citrullus lanatus*), and jamun fruit (*Syzygium cumini*) were rinsed under running water. The segments were finely minced, and the fruit pulp was removed from the seeds. The juice was filtered out after 100 grams of minced pulp were mashed using a pestle and mortar. The outer green covering was removed from the watermelon (*Citrullus lanatus*) to access the interior. Following separation of the fruit's pulp and seed, the pulp was removed, crushed in a pestle and mortar, and filtered. The outer portion of the green layer was removed to create the aloe vera gel's interior. For this synthesis, the gel's core was roughly crushed to form a thin, uniform jelly. Using watermelon, jamun, and aloe vera gel extracts as fuels, MgO nanoparticles were produced *via* bio-mediated combustion. A muffle furnace preheated to 450 ± 5 °C is used to hold the mixture after 1.4 g of high-purity magnesium nitrate ($Mg(NO_3)_2$) has been dissolved in 10 ml of water and 5 ml of plant extracts, and the mixture has been stirred with a magnetic stirrer for 15 minutes. After that, the mixture is moved to a Petri dish. The entire reaction took less than five minutes, and to improve the sample's phase and crystallinity, it was calcined for two hours at 600 °C.[97,98] Additionally, spherical Zn^{2+}-doped MgO nanoparticles were made using aloe vera latex extract as green media in a simple, affordable, and environmentally friendly manner. To make the nanomaterial, aloe vera was extracted by boiling it with ethanol and water, adding it to a solution of $MgCl_2$ and $ZnCl_2$, precipitating it with ammonia, and then calcining it. The process creates green nanomaterials without the need for further purification by using bio-extracts as stabilizing and reducing

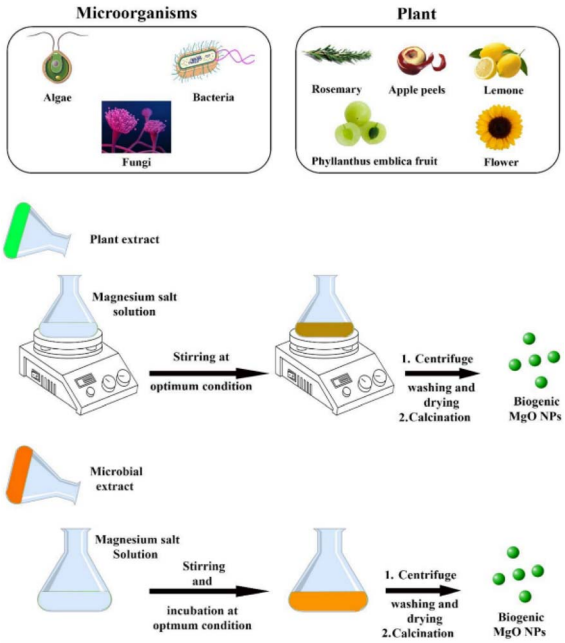

Fig. 6 Describes two biogenic synthesis pathways that use natural extracts rather than harsh chemicals to produce MgO NPs. Reproduced under terms of the CC-BY license from ref. 84. Copyright 2017, Marzieh Ramezani Farani, published by *Catalysts*.

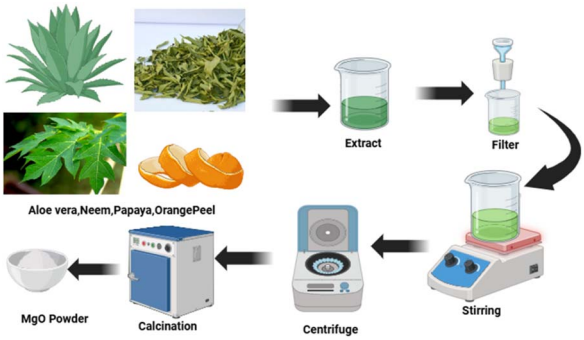

Fig. 7 Represents the GS of MgO NPs using a variety of plant resources.

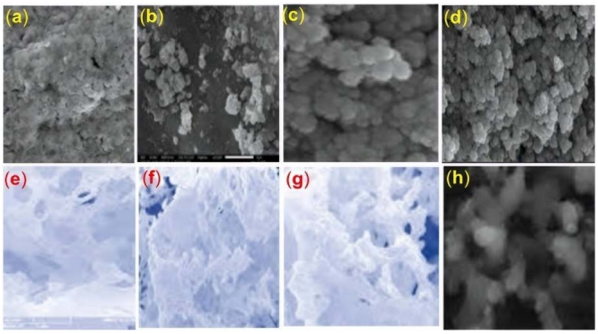

Fig. 8 Represents the comparative SEM images (a–h) of MgO NPs synthesized *via* green routes and doping techniques. (a) Reproduced under terms of the CC-BY license. Copyright 2017, Abdul Muhaymin, published by *Scientific Reports7*.[77] (b) Reproduced in accordance with the CC-BY license. Reproduced under the conditions of the CC-BY license. Copyright 2017, R. Supreetha, Elsevier.[94] (c) Ain Farina Farizan, published by Springer Nature, copyright 2017.[95] (d) Taken from ref. 96. Copyright 2017, Elsevier, Enobong R. Essien. (e–g) Reproduced using the CC-BY license. Copyright 2017, Lavanya Ramakrishna, Elsevier.[97] (h) Reproduced using the CC-BY license. Rajeshwari B. Rotti, published by Frontiers, copyright 2017.[29]

agents.[99] Ag-doped MgO nanoparticles were made by co-precipitating silver nitrate and magnesium nitrate in distilled water and regularly adding plant extract. To create off-white MgO NPs and light grey Ag NPs, the solution was centrifuged, cleaned with alcohol, dried, and calcined at 350 °C after its color changed. The resulting nanoparticles were stored in airtight containers for future use and demonstrated a simple and eco-friendly production procedure.[98,100,101]

Neem served as a fuel and a reducing agent in the synthesis of CuMgV NPs. CuMgV NPs were prepared by burning. Stoichiometric calculations were based on the compounds' total reducing and oxidizing valences. First, 1.24 g of Cu $(NO_3)_2 \cdot 3H_2O$, 1.27 g of Mg $(NO_3)_2 \cdot 6H_2O$, and 0.57 g of NH_4VO_3 were dissolved in 10 ml of water. Next, 0.9 g of gasoline was added to the mixture. A magnetic stirrer was used to agitate the combined liquids for around ten minutes. To create single phase copper magnesium vanadate, this homogenous mixture was evaporated for 10 to 15 minutes at 540 ± 10 °C in a muffle furnace. The end product was a black powder that produced large amounts of gases, including CO_2, N_2, and H_2O, after three hours of calcination at 750 °C. Fig. 9,[97,102,103] shows how different biowastes can be burned to produce MgO. Co–MgO nanoparticles were made by dissolving cobalt and magnesium nitrates in *Azadirachta indica* leaf extract. After that, the mixture was agitated at 70 °C while NaOH was gradually added to maintain pH. The reaction mixture was cleaned, centrifuged, and agitated several times before being dried and annealed to create crystalline nanoparticles. This green co-precipitation method uses plant extract as a capping agent to produce controlled, eco-friendly nanomaterials.[104,105] Watercress and spinach extracts were used as reducing agents for $KMnO_4$ to produce MgO NPs in a straightforward, environmentally friendly synthesis. The fresh spinach and watercress were chopped, cleaned, boiled, and filtered in order to create extract solutions. The watercress extract solution was added dropwise to a solution of 3 g $KMnO_4$ acidified with 2.5 M H_2SO_4 to create the sample MW. The liquid turned black after an hour of stirring at room temperature, indicating that the watercress extract had totally reduced $KMnO_4$. Following filtration, the black precipitate was dried for a whole night at 100 °C after being frequently washed with distilled water. After that, the black powder was calcined at 300 °C for five hours at room temperature. MS was replaced with spinach extract, but otherwise the identical process was carried out.

Most plant extracts contain phytochemicals, or bioactive compounds, such as proteins, tannins, alkaloids, polyphenols, flavonoids, and carboxylic acids. These substances act as capping and reducing agents by decreasing metallic ions from (M^+) to (M^0) *via* an oxidation/reduction mechanism. A color

shift in the reaction mixture indicates that the reduced metallic state has formed into clusters of nanoparticles.

Because it eliminates dangerous chemicals and generates less toxic waste, green synthesis for nanoparticles has the benefits of being sustainable and environmentally benign. It can be done at room temperature, is economical, and can produce large quantities. It can also produce nanoparticles with improved characteristics, like greater stability and particular surface characteristics, and result in more biocompatible goods.

The sol–gel approach for producing MgO NPs has the drawback of requiring extremely precise control over pH, temperature, and humidity because even little changes can change the size and structure of the particles. Agglomerated nanoparticles may occur if stabilizers or surfactants are not used, and long reaction times are another disadvantage of this method. Additionally, several of the precursors and solvents used are costly or hazardous, making it difficult to scale up the process for industrial manufacturing. Similarly, there are some disadvantages to the co-precipitation method of producing MgO nanoparticles.[57] High-temperature post-calcination is frequently required, which may result in uneven particle sizes, particle growth, and a decrease in surface area. Precise management is essential because variations in pH and reaction rate may lead to the formation of contaminants and complex doping method are not possible for this method. In hydrothermal process of producing MgO NPs, take a long time of synthesis, and high-temperature, high-pressure equipment is required, not produced large-scale production, difficulty of controlling particle aggregation. Furthermore, several of the solvents used in this procedure may be hazardous. There are several drawbacks to burning or combustion as a method of producing MgO NPs. Even though inhomogeneous heating may produce heterogeneous particle sizes, the high temperatures involved may cause particle sintering and a loss of nanoscale characteristics. Controlling the form and porosity of nanoparticles can frequently be challenging, and some of the precursors utilized in this process may be hazardous or explosive. Using a microwave-assisted method to produce MgO NPs has a number of drawbacks. Rapid heating can result in non-uniform nucleation, which can lead to variances in particle size, and the equipment needed is more costly than with traditional heating methods. This approach is usually limited to small-scale synthesis unless specialized industrial microwave reactors are used. Reaction parameters need to be carefully adjusted in order to obtain correct results. Fig. 10 illustrates the four main areas of nanoparticle synthesis constraints: material, synthesis method, nanoparticle (NP) quality, and application. Some of the major challenges include restricted plant dispersion and seasonal availability, high-temperature and high-pressure synthesis requirements, low yield and irregular particle morphology, and limited removal efficiency and application conditions. Together, these problems lead to increased energy consumption, increased production costs, lower-quality products, and practical difficulties in real-world applications.[106] Lack of raw materials, irregular and variable particle sizes, low yields, and lengthy reaction periods are common drawbacks of green synthesis. Additionally, the biological components might be difficult to deal with and scale up, necessitating specialized, repeatable, and affordable technology to produce reliable outcomes.[107]

Long processing times are needed to produce MgO NPs using the sol–gel method, especially during the gel formation and drying stages that follow. Furthermore, the overall cost of manufacturing is frequently increased by the use of expensive chemical solvents and precursors. Furthermore, the sol–gel process is less practical for large-scale manufacturing due to the substantial difficulties in scaling up to industrial levels.[61,62] The ecologically safe synthesis of magnesium oxide nanoparticles from plant extracts is hampered by a number of factors. First, variations in the amount of plant extract could cause irregularities and jeopardize the consistency of the synthesis of nanoparticles. Complex macromolecule extracts could make the purification process more difficult. Furthermore, compared to physical synthesis techniques, green synthesis methods offer less control over the particle size distribution.[63–65]

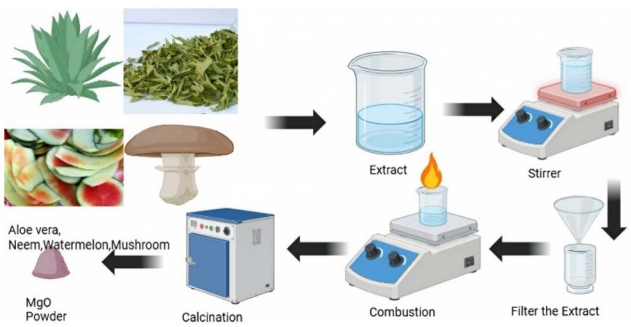

Fig. 9 Demonstrates a green synthesis route for MgO NPs using plant and fungal extracts such as aloe vera, neem, watermelon, and mushroom.

4 Applications of MgO NPs in various fields

MgO NPs enable a wide application due to their high surface area, biodegradability, and biocompatibility. Focusing on the agriculture sector, they elevate plant growth and restrict the disease by improving water absorption and activating key enzymes such as amylase and protease, which are essential for seed germination. Therefore, they acted as fertilizer sources, soil supplements, and animal feed additives. Owing to their antibacterial and antifungal properties, MgO NPS are used in wound dressings, dental materials, and medical device coatings, where they degrade microbial membranes and generate reactive oxygen species to prevent infections and promote faster recovery. MgO NPs are effective catalytic supports in the production of chemicals and propellants due to their stability, high temperatures, and abundance of active sites for chemical reactions. By improving the charge capacity and cycling durability, dielectric characteristics, and nanoscale structure, it can be used in energy storage of supercapacitor electrodes.

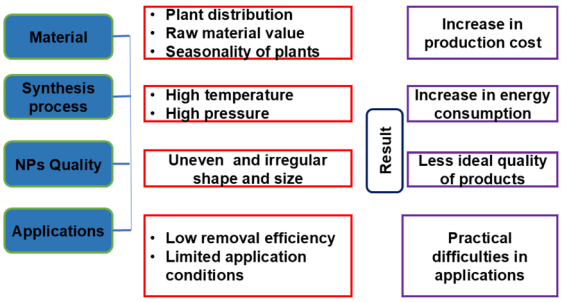

Fig. 10 Represents the constraints of nanoparticle synthesis *via* green approach.

4.1 Magnesium oxide applications in the realm of agriculture

Magnesium is an important macronutrient that helps chlorophyll-based photosynthesis, which fortifies plants and boosts agricultural output by improving the absorption of needed minerals such as phosphorus and nitrogen. It maintains cell wall integrity and stimulates the enzymes required for large yields for fruit development and flowering. The admirable properties of MgO NPs, such as low phytotoxicity, thermal stability, non-genotoxicity, and non-biotoxicity to humans, have attracted significant interest in the field of agriculture. Also, it is highly advantageous for plant protection due to these characteristics[108] They have demonstrated efficacy in stimulating plant and seedling growth, particularly in crops such as peanuts.[92,109,110] In agricultural lime, MgO aids in improving soil structure and aeration, lowers acidity, and strengthens root systems. MgO's dominant antibacterial and antifungal properties help reduce soil-borne diseases, reducing the need for synthetic pesticides and promoting organic, sustainable farming methods. The flowchart for MgO NPs in an agricultural setting is shown in Fig. 11. By functioning as synthetic fertilizers to increase crop output and as nano pesticides to control pests, weeds, and diseases, green-synthesized MgO NPs hold further potential for sustainable agriculture.[111–114] Their dual role has been extensively researched and recorded, and by lowering infection rates and biofilm formation, inhibits *Ralstonia solanacearum*, a dangerous tobacco disease.

These findings were corroborated by greenhouse experiments, which showed increases in plant biomass and height after treatment. In addition to controlling pathogens, MgO NPs coated on cotton fibers have been applied to disease management, phytoremediation, nanopesticide administration, and seed germination.[115] It can be included in agricultural textiles that provide UV protection in addition to crop protection. The Ultraviolet Protection Factor (UPF) of coated textiles exceeds 50, which is considered exceptional for protecting against damaging radiation. These textiles are functional for horticulture, floriculture, and other agricultural uses, such as mulching, insect and bird netting, and shade nets, especially in areas with high levels of sunlight, which increase productivity and protect plant health, and they have great potential in soil consolidation, especially when incorporated into cotton and coir fibers, as they extend the lifespan of soil components and reduce plant water absorption by about 170%. When bamboo fibers were combined with MgO, the soil's strength and stiffness improved significantly, particularly at a fiber content of 1.2%.[114,116–118] Deeper understanding of the absorption, transport, and bioactivity of MgO NPs is the goal of ongoing research, which will help ensure their safe and efficient use in food systems of the future.[118,119] The tensile strength and durability of fibre-based agricultural materials used in infrastructure or soil stabilization are improved, beneficial microbial activity is encouraged, and crop tolerance to biotic and abiotic stresses is increased thanks to MgO NPs. Beyond crop support, their significance is further enhanced by their high stability, environmentally favourable profile, and capacity to reduce heavy metal toxicity and promote sustainable pavement subgrades, making them important for next-generation agricultural sustainability and infrastructure solutions.[120,121]

4.2 Applications of MgO in the environment

Compared to relative studies, it can do better than traditional fertilizers and pesticides due to their improved bioavailability, reduced application rates, and extended nutrient release, all of which improve crop health and reduce environmental impact. To obtain more precise, effective resource use and reduced chemical runoff, MgO NPs are increasingly employed in contemporary precision agricultural technologies for targeted distribution *via* foliar sprays, soil additives, or seed coatings. According to safety and environmental impact studies, green-synthesized MgO NPs are ideal for open-field applications because they decompose into harmless magnesium salts, exhibit low ecotoxicity, and don't harm non-target animals or soil microbes.[122–124] In addition to treating water and soil, MgO NPS have great potential for adsorbing gaseous pollutants and purifying air. Acidic gases and volatile hazardous compounds, such as sulfur oxides (SO_x) and nitrogen oxides (NO_x)which are major contributors to air pollution and acid rain, are strongly attracted to these nanoparticles. Due to their surface reactivity and stability, they can act as highly effective adsorbents, or "sponges," capable of capturing,

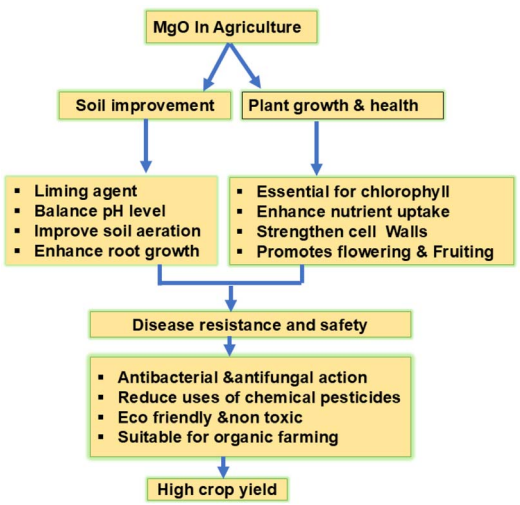

Fig. 11 Illustrates the benefits of MgO NPs in agriculture or tilling.

neutralizing, or decomposing these toxic gases into less hazardous ones[125–129]. Recent studies have shown that adding MgO NPs to diesel engine systems can significantly reduce emissions of carbon monoxide (CO) and nitrogen oxides (NO_x), two of the most prevalent and dangerous vehicle pollutants. Compared to many conventional chemical adsorbents and scrubbers, which may pose secondary environmental risks or pose degradation challenges, magnesium oxide nanoparticles offer a safer, more environmentally friendly, and biocompatible alternative. Because of their usage in air filtration systems, vehicle exhaust purification, and industrial flue gas treatment all of which show their growing importance in regulating urban and industrial air quality they are a crucial part of the fight against airborne environmental pollution.

One of the most notable environmental applications of magnesium oxide nanoparticles is the control of industrial wastewater, especially in industries known to produce complex, toxic effluents. The effective use of the *Aspergillus carbonarius* strain D-1 to produce green-synthesised MgO NPs as adsorptive and catalytic coatings for textile materials. These coated textiles showed remarkable efficacy in pulling out pollutants when subjected to carefully controlled conditions, including temperature, pH, contact time, and precursor concentration. They specifically showed a 97.5% decrease in COD and an outstanding elimination of heavy metals as nickel, cadmium, lead, and chromium (87.06%).[83] By significantly reducing the pH, total dissolved solids (TDS), total suspended solids (TSS), and electrical conductivity of the treated water, these materials also demonstrated their capacity to detoxify and change important industrial pollutants. Analytical methods such as GC-MS further supported the effectiveness of these nanoparticles in thoroughly cleaning wastewater by confirming the breakdown and reduction of organic pollutants in the effluent. MgO NPs are a popular choice for businesses seeking to implement cleaner production methods while complying with environmental standards due to their low toxicity, affordability, and reusability. These developments establish MgO based nanotechnologies as essential elements of contemporary environmental engineering and environmentally friendly industrial wastewater treatment.[130–132] Because of its special qualities, such as having the necessary surface basicity that results in the formation of oxygen vacancies that impact the CO_2 absorption capacity, MgO is a viable adsorbent substitute for CO_2 capture applications.[133] MgO has a clear advantage over other metal oxide adsorbents, like those based on Li and Ca, because it requires a lower regeneration temperature. Furthermore, MgO's high theoretical adsorption capacity of 24.8 mmol CO_2 g^{-1} makes it a viable adsorbent for CO_2 capture at the intermediate temperature range of 473–673 K.[134] Fluoride (F)-contaminated water has become a major global issue in recent years. The WHO recommends that the amount of F ions in drinking water be less than 1.5 mg L^{-1}. Many bone disorders, including osteoporosis, arthritis, and dental and skeletal fluorosis, are brought on by an excess of fluoride ions in drinking water.[135] The breakdown of fluoride-containing minerals and the discharges from businesses that use a lot of fluorochemicals, like electroplating, semiconductor manufacture, cosmetics, ceramics, and aluminium smelting, allow fluoride ions to enter and damage the water system.[136] Therefore, a workable solution for removing fluoride ions from contaminated water needs to be created. Fluoride ions have been extracted from water using a variety of techniques, including nanofiltration membrane, precipitation, adsorption, reverse osmosis, and ion-exchange.[137]

Adsorption is found to be the most widely used and preferred approach among them due to its simple operation, low cost, and highly effective methodology.[138] Nano-sized metal oxides for defluorination, such as Fe, Mn, Al, Ti, Ca, Mg, and Zr oxides, are described in the literature. Moreover, it has been shown that rare earth metal oxides have strong sorption abilities to eliminate F ions. These metals can be employed as single oxide adsorbents, notwithstanding their high cost. According to reports, MgO is an excellent adsorbent for defluorination, because of their high surface hydroxyl groups, enhanced sorption capacity, non-toxicity, affordability, and environmental friendliness, MgO NPs have been shown to be a very effective nanoadsorbent for eliminating fluoride from wastewater. The most emphasis has been paid to research on iron and magnesium-based nanoparticles as a way to get rid of fluoride. One of the most commonly reported gaseous contaminants in the environment is hydrogen sulfide (H_2S).[139] The neurological system, respiratory system, reproductive system, eyes, skin, cardiovascular system, hepatic tissues, renal system, gastrointestinal system, immune system, and endocrine system are all negatively impacted by H_2S poisoning. The elimination of H_2S has been found to be catalyzed by both MgO and $Mg(OH)_2$. According to several studies, MgO removes H_2S by chemically adsorbing HS and S onto flat MgO surfaces since H_2S has a weak direct contact with MgO. Furthermore, metal oxides by themselves can only adsorb H_2S at high temperatures. Researchers attempted to boost the sorbent's capacity at room temperature by experimenting with various methods, such as adding tiny MgO into a porous matrix like activated carbon. This would make it possible to employ both chemical and physical H_2S adsorption. Therefore, in industrial applications, it will be a better choice than using metal oxide alone to remove H_2S from contaminated gas streams. To the best of our knowledge, no research has been conducted to assess the composite's ability to catalyze H_2S using micro MgO and GAC.[140,141]

Wastewater from companies and everyday living releases metal ions, which are a serious issue for the ecology. When people or other living things unintentionally drink water tainted with these metal ions, they may have serious health issues. As a result, identifying metal ions in water aids in the advancement of wastewater and tap water treatment technologies.[142] Thermoelectric atomic absorption spectrometry, flame atomic absorption spectrometry, and inductive plasma mass spectrometry are some of the techniques used to identify metal ions. These techniques are vulnerable, but the equipment is costly, complicated, and requires advanced technical knowledge to operate.[143] An alternative and promising method for detecting metal ions is the use of green NPs. Measuring the capacity to identify metal ions in water depends on MgO NPs capacity to bind metal ions.[144] Selected *S. aromaticum* flower extract to create MgO nanoparticles for colorimetric Fe^{3+} detection. As

a result, in the presence of 14 other interfering metal ions, such as Ca^{2+}, Cd^{2+}, Co^{2+}, Cu^{2+}, Hg^{2+}, and Fe^{2+}, the limit of detection was obtained at 23 μm at a concentration five times greater than that of Fe^{3+}. Lead in water can be detected by MgO NPs in addition to Fe^{3+}. Lead is a known toxic substance that can be hazardous to humans and other living things also it is colorless, odorless, and difficult to detect in aquatic environments. In certain regions, children's blood Pb^{2+} levels were found to be higher than the acceptable threshold, averaging 1.00 μg L^{-1}.[145] According to research[146] MgO NPs using *S. aromaticum* flower extract can detect Pb^{2+} with a detection limit of roughly 24 μm. In order to detect a drop in the fluorescence intensity of the MgO nanoparticles, this investigation was conducted at pH 3. This could be because, at this pH, Pb^{2+} ions interact specifically with MgO NPs, but other metal ions do not. One use for MgO NPs is the detection of hazardous substances in liquefied petroleum gas. Liquefied petroleum gas is extensively utilized in industrial, commercial, transportation, and civil purposes, particularly in urban and rural homes for cooking. They will transform into gas when they get out of the container, which makes storage challenging. Furthermore, even in little amounts, these basic ingredients can catch fire and explode when they leak. Green produced NP, particularly MgO nanoparticles, are gradually demonstrating their ability to provide advantages over other traditional gas sensing technologies. In fact, used aloe leaf extract to create MgO NP-based liquefied petroleum gas sensors, with the greatest sensitivity percentage of 38% for 1000 ppm of LPG.[147]

4.3 Applications of MgO that are antibacterial and antimicrobial

The antibacterial mechanism of MgO nanoparticles has been explained by a number of mechanisms, including the production of reactive oxygen species (ROS), the contact of nanoparticles with bacteria, which damages the bacterial cell, and an alkaline impact. The inhibitory impact of silver nanoparticles on bacteria has been explained by a number of comparable processes. It has long been recognized that silver inhibits microorganisms. One of silver's antibacterial processes is the stimulation of oxidative stress brought on by the production of ROS, which may lead to the breakdown of the cell's membrane structure. It has been documented that the release of ions from the surface of nanoparticles can kill bacteria by attaching to their cell membrane.[148,149] Numerous studies have shown that the production of ROS, such as superoxide anion (O_2^-), is responsible for the antibacterial mechanism of MgO nanoparticles.[84,150] According to reports, an increase in the surface area of MgO particles raises the concentration of O_2^- in solution, which makes it easier to destroy the bacterial cell wall. However, because of the extremely high surface energy of the particles, the aggregation effect becomes quite important when the MgO particle size is less than 15 nm. The bactericidal efficacy decreases because of the huge size of aggregated MgO, which prevents contact with bacteria and particles.[151] According to research,[29] the surface of MgO powder produced a significant amount of O_2^-, which enhanced the antibacterial activity of MgO nano powder against *E. coli*. The antibacterial activity of MgO nanoparticles against the Gram-positive bacterium *S. aureus* and the Gram-negative bacteria *E. coli* and *Pseudomonas aeruginosa* (*P. aeruginosa*) was recently assessed by ref. 152. With a minimum inhibitory concentration (MIC) of 500 μg ml^{-1} for *E. coli* and 1000 μg ml^{-1} for *P. aeruginosa* and *S. aureus*, MgO nanoparticles demonstrated antibacterial activity.

Due to oxygen vacancy flaws on the surface of the nanoparticles, it was proposed that lipid peroxidation and ROS could be the mechanism of MgO NPs antibacterial action. It has been suggested that MgO NPs antibacterial activity is explained by their contact with bacteria, which damages the bacterial surface. Because of the interaction between particles and bacteria, it has been shown that nano-MgO exhibited great activity against bacteria. Because of their surface defects and positive charge, it was discovered that nano-MgO particles could absorb halogen gasses. This led to a significant interaction with negatively charged bacteria. Another important component of MgO nanoparticles' antibacterial activity has been identified as the alkaline effect. The adsorption of aqueous moisture on the surfaces of MgO nanoparticles, which might create a thin layer of water surrounding the particles, was suggested as a potential antibacterial mechanism. This thin layer of water surrounding the nanoparticles may have a local pH that is significantly higher than its equilibrium value in solution. The high pH in this thin layer of surface water could harm the membrane and cause cell death when the nanoparticles come into contact with the bacteria.

MgO NPs have emerged as strong antibacterial agents, well-suited for applications in food packaging, healthcare, and sanitation. The hunt for alternative antibacterial remedies has accelerated amid growing concerns about bacterial mutations, frequent pathogen outbreaks, and antibiotic resistance. Reactive oxygen species (ROS), including hydrogen peroxide (H_2O_2), superoxide ions (O_2^-), and hydroxyl radicals ($^{\bullet}OH$), are the main way that MgO NPs produce their antibacterial actions.[153,154] By attacking bacterial cells and disrupting essential biological functions, these ROS oxidize membrane lipids, denature proteins, and damage DNA to increase their bactericidal activity. Lipid peroxidation caused by oxygen vacancies in MgO is required due to their large surface area. MgO NPs exhibit strong electrostatic interactions with bacterial membranes, leading to structural damage and intracellular content leakage. Additionally, they are more affordable, safer, chemically stable, and have broader-spectrum antibacterial activity than more traditional agents such as silver.[155,156] MgO nanostructures produced using a variety of methods, including sol-precipitation (SPT), sonochemical (ST), precipitation (PT), chemical combustion (CC), and microwave combustion (MWC), were evaluated for their efficacy against Gram-positive *Staphylococcus aureus* and Gram-negative *E. coli*. The MgO NPs produced using the SPT, ST, PT, and CC procedures performed quite poorly, whereas those made using the MWC method had the strongest antibacterial activity.157[157] It was found that *S. aureus* was more susceptible than *E. coli* due to structural differences in its cell wall. Gram-positive bacteria have a strong peptidoglycan layer without an outer membrane, making them

more vulnerable to MgO damage. However, because of their more complex outer membrane and structure, Gram-negative bacteria are less vulnerable. These results were supported by experimental research showing that *S. aureus* had larger zones of inhibition than *E. coli*.[158]

The antibacterial activity was found out using the agar well diffusion method, and using sterile cotton swabs, freshly prepared bacterial inoculums were evenly distributed over nutrient agar plates. Then, 10 μg ml^{-1} of M1, M2, ampicillin, and water (negative control) were added to four separate wells. After a 24-hour incubation period at 37 °C, the zones of inhibition were observed. Each test was done three times to make sure reproducibility. Interestingly, MgO NPs significantly outperformed bulk MgO in antibacterial activity against *R. solanacearum*, even at a low concentration (250 μg ml^{-1}). After adhering to the bacterial cell walls and undergoing structural breakdown, the nanoparticles finally penetrated the cells, causing cytoplasmic leakage and ultimately cell death. Oxidative stress, physical membrane rupture, and possibly genotoxic consequences, including DNA fragmentation, are all part of the mechanism of action. Additionally, MgO NPs prevented bacteria from swimming and twitching, suggesting a reduced ability to infect and form biofilms. Overall, the effectiveness of MgO NPs in killing bacteria is directly influenced by their shape, particle size, and surface area. They are also appealing choices for controlling microbial contamination and diseases because of their small size, which raises the generation of reactive oxygen species and surface reactivity. In recent research, Ppy–MgO and PPy–MgO–carbon nanotube (CNT) composites were prepared *via in situ* chemical polymerization. With inhibition zones of 4.0 mm and 3.0 mm, respectively, the ppy–MgO–CNT composite demonstrated antibacterial activity against MRSA and PAO1 and had a UPF of 30.[159] NPs incorporated textile materials are becoming increasingly popular due to their many uses, including self-cleaning, UV protection, and medical applications. Because of their high moisture-retention capacity, textile surfaces, particularly those composed of natural fibers like cotton, frequently serve as microbial growth reservoirs in hospital settings. Hospital-acquired infections can be considerably decreased by using antimicrobial compounds in textiles.

Metal oxide nanoparticles, such as TiO_2, ZnO, MgO, and CaO, are commonly utilized in textiles due to their strong antibacterial properties, chemical inertness, and lack of toxicity to humans and animals. Among them, MgO NPs are suitable because of their stability and ability to penetrate bacterial cell membranes.[160,161] Recent research has focused on embedding MgO NPs into bio-composites for wound dressings. To develop concepts like antibacterial biofilms, polyvinylidene fluoride (PVDF) has been combined with MgO (3–7 wt%) using methods such as spin coating and electrospinning. These bioactive, piezoelectric materials not only prevent infection at the wound site but also function as smart wound-healing sensors by responding to external stimuli. MgO NPs can disrupt bacterial and fungal cell walls; they display strong antibacterial properties. There are two important mechanisms responsible for microbial death: membrane leakage and the generation of reactive oxygen species (ROS). This property is particularly useful in treating food-borne infections such as *Escherichia coli* and *Salmonella enteritidis*. Even at low concentrations, MgO NPs have demonstrated effectiveness against these bacteria, which are known to cause severe gastrointestinal disorders in humans. Their large surface area and high reactivity enable enhanced interaction with microbial cells, making them effective antibacterial agents in food safety applications. MgO NPs are suitable for use as disinfectants, packaging materials, and food-contact surfaces, as they can function under various environmental conditions without producing harmful byproducts. Furthermore, nanoparticles have shown remarkable antibacterial activity against phytopathogenic microbes that cause devastating crop diseases. One example is their impact on *Acidovorax oryzae*, the bacterium that causes bacterial brown stripe in rice. Using the green plant extract were able to successfully synthesis MgO NPs, which demonstrated a robust inhibitory impact on this pathogen. Furthermore, *Ralstonia solanacearum*, the cause of bacterial wilt in numerous crops, has been successfully combatted by MgO NPs. MgO nanoflowers, specifically organized nanoforms, were developed in recent research to improve antibacterial efficacy significantly. So nanostructures provide high surface area and more active sites for microbial interactions; they are more effective at suppressing harmful bacteria. These kinds of developments suggest a non-toxic, sustainable method of crop protection that enhances plant health and reduces the use of chemical pesticides.[162–165] Fig. 12 illustrates the antibacterial activity of MgO NPs. It has shown promising efficacy against biofilms, bacterial communities that are highly resistant to standard antibiotics and disinfectants. Examples of these communities include those found on food surfaces, medical equipment, and environmental reservoirs. MgO NPs are useful for preventing chronic infections, reducing hospital-acquired contamination, and enhancing food safety because they interfere with biofilm formation and maintenance. Recent research also shows that they work well against antibiotic-resistant bacterial strains and can be incorporated into dental and oral hygiene products to reduce infections and tooth plaque. To broaden the spectrum of activity and enhance synergistic antibacterial effects, researchers are now investigating MgO NPs in combination with other nanomaterials or polymers. Because of these characteristics, magnesium oxide nanoparticles are an essential aspect of cutting-edge antimicrobial technology for the food sector, healthcare, and environmental safety.[165,166]

The antibacterial activity of MgO NPs and ZnO NPs against the bacterial strains of *Staphylococcus aureus* (ATCC6538), *Bacillus subtilis* (ATCC6633), *Listeria innocua* (CLIP74915), *Pseudomonas aeruginosa* (ATCC9027), and *Salmonella typhimurium* (ATCC14028) was tested using the agar well diffusion method.[166] Using sterile rods, 100 μL of the 24-hour matured bacterial strain broth culture was swabbed onto the prepared nutritional agar plates. A sterile cork borer was used to produce a 6 mm well in each Petri plate. The bactericidal properties of ZnO NPs and MgO NPs were investigated using solutions containing 2, 4, and 6 mg ml^{-1}. The solutions of both nanomaterials were prepared in a 10% (v/v) DMSO solution and applied to the wells using sterile micropipettes.

The antibacterial activity of MgO NPs and ZnO NPs was evaluated using Gram-positive bacteria (*Staphylococcus aureus*, *Bacillus subtilis*, *Listeria innocua*) and Gram-negative bacteria (*Pseudomonas aeruginosa*, *Salmonella typhimurium*). The culture plates were prepared using a sterilized glass rod and streaked with 100 L of the corresponding bacterial strains' 24-hour matured broth culture. Each Petri plate has six 6 mm wells created using a sterile cork borer. MgO and ZnO nanoparticles were suspended and present in Dimethyl Sulfoxide (DMSO) at varying concentrations (2, 4, and 6 mg ml^{-1}). Each experiment was run three times. Both ZnO NPs and MgO NPs demonstrated exceptional antibacterial activity against the investigated bacterial strains, with the exception of *Staphylococcus aureus*. *Bacillus subtilis* (17 ± 0.35 mm) and *Salmonella typhimurium* (10 ± 0.19 mm) displayed the highest and lowest inhibitory zones, respectively. However, it was demonstrated that the NP concentration affected the detected antibacterial activity. In general, the emergence of drug-resistant bacterial strains required the invention of a new class of potent antibacterial medications. ZnO NPs are generally thought of as stable and harmless antibacterial agents because they basically don't harm humans or animals. ZnO NPs have antibacterial qualities because of the release of reactive oxygen species (ROS) from their surface. This causes oxidative stress by damaging cell membranes, cellular proteins, and DNA when it comes into contact with bacterial cells and accumulates in their microorganisms. By releasing antimicrobial ions (Zn^{2+}) inside the cells, these NPs create a toxic milieu that damages the membrane and intracellular space.[167]

4.4 Versatile heterogeneous base catalyst in industrial

Because of its surface basic sites, which promote important chemical processes such as deprotonation and nucleophilic attacks, it is a well-known solid base catalyst. The strength and density of the catalyst can be precisely controlled thanks to these sites, which are predominantly O^{2-} anions and are highly tunable through changes in synthesis techniques, calcination temperature, and particle size. MgO is essential for medicines, agrochemicals, and biofuels because it is particularly effective in base catalyzed processes such as transesterification, aldol condensation, and Michael addition. MgO is compared to homogeneous base catalysts like NaOH or KOH, it offers significant benefits due to its thermal stability, affordability, and non-toxicity, facilitating simpler separation and recycling. These qualities make MgO highly attractive for industrial-scale applications where reliance and strong catalysts are vital. The most extensively studied catalytic role of MgO in biodiesel production is the transesterification of triglycerides with methanol.[168] Unlike conventional catalysts, which often cause problems with soap formation and purification, MgO is a heterogeneous catalyst that can be recovered and reused without significant loss of activity. Due to their increased surface area and enhanced basicity, nanosized MgO NPs further improve this efficiency by inducing reaction rates and yield. In addition to biodiesel production, it is also used catalytically in oxidation and dehydrogenation reactions, particularly in petrochemical processes such as the conversion of ethanol to acetaldehyde. Fig. 13(a) illustrates the antibacterial properties of MgO nanoparticles and Fig. 13(b) the catalytic role of MgO in the dehydrogenation of secondary alcohols to ketones.

MgO NPs effectively facilitate waste-to-fuel conversion, CO_2 fixation, and pollutant degradation, thereby supporting sustainable and eco-friendly chemical processes. It enhances the stability and dispersion of metal catalysts such as Pt, Pd, and Co, especially in steam reforming and OCM processes.[35] And the interaction between MgO and these metals can substantially affect catalyst lifetime and reaction selectivity, both of which are critical at elevated temperatures. Owing to their exceptional surface reactivity, strong basicity, and thermal stability, MgO NPs have emerged as promising materials for green catalysis and advanced chemical synthesis. By promoting pollutant degradation, CO_2 fixation, and waste-to-fuel conversion, these nanoparticles effectively contribute to the advancement of sustainable and eco-friendly chemical technologies.[169–172]

Recent research has shown the effectiveness of MgO-based catalysts across a wide range of sustainable chemical transformations, the depolymerization of PET and other plastics, the conversion of biomass-derived compounds into valuable chemicals, and the production of biodiesel from used cooking oil. MgO is suitable for both batch and continuous-flow applications due to its large surface area and adjustable basicity.[157] Its operational stability enables multiple reuses with minimum loss of activity, thereby decreasing the costs and dedicating safe environmental sustainability. In complex industrial reactions, MgO can also be doped or modified with additional metals (such as Ca, Al, or Ce) to improve its selectivity, catalytic activity, and resistance to deactivation. Nowadays, MgO NPs are seen as an essential component of next-generation green catalysis (b), assisting with sustainable industrial processes and circular economy projects.[173–176]

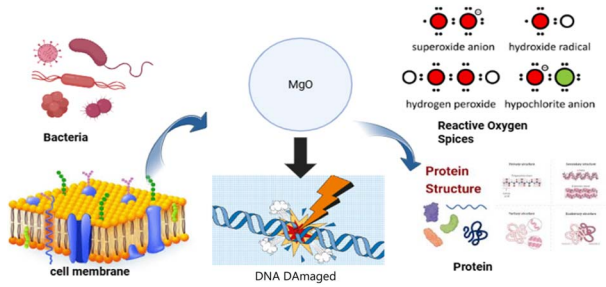

Fig. 12 Depicts how MgO nanoparticles exert antibacterial effects by attacking multiple bacterial targets.

4.5 MgO in supercapacitor applications

MgO's distinct physicochemical properties such as its high surface area, changeable porosity, and exceptional chemical and thermal stability, have made it a viable material for supercapacitor applications. The abundant and environmentally safe MgO provides an affordable option for large-scale energy storage devices. Its surface is full of basic O_2^- sites

that enhance capacitive behaviour and ion adsorption from electrolytes. High-rate charge–discharge cycles in supercapacitors require more active sites and shorter ion diffusion pathways, which are provided by the nanostructured form of magnesium oxide, such as nanoparticles, nanorods, and nanoflakes, which further enhances its electrochemical performance.[177] A general property of MgO is low electrical conductivity, which restricts its use as an electrode material, and to overcome this, researchers have been combining MgO with highly conductive substances such as reduced graphene oxide (rGO), conducting polymers, and carbon nanotubes (CNTs) to create composite materials. These hybrid structures take advantage of MgO's dielectric properties for enhanced energy storage, while the conductive matrix facilitates faster electron transport. For instance, MgO/rGO composites have demonstrated improved specific capacitance and cyclic stability, with rGO ensuring efficient charge transfer and MgO providing a large surface area. The electrochemical performance of MgO is escalated when combined with pseudocapacitive compounds, as MgO–MnO_2 and MgO–NiO composite electrodes exhibit higher energy and power densities than their pure counterparts, as shown in studies. In these composites, the redox-active transition metal oxides and the structural support provided by MgO work synergistically to enhance electrical conductivity and ion transport, resulting in increased specific capacitance and better rate capability. In addition, MgO increases the cycle stability of supercapacitors by acting as a buffering matrix that prevents volume expansion and structural degradation during prolonged charge–discharge cycles. Recent innovations in synthesis approaches, especially in green synthesis using plant extracts and combustion methods, have been explored to produce MgO nanostructures with improved supercapacitor performance. These environmentally friendly and safe synthesis routes not only reduce ecological impact but also introduce surface functional groups that enhance wettability and electrolyte interaction. When used in supercapacitors, green-synthesized MgO NPS have demonstrated promising electrochemical stability and cycle-life retention, highlighting their potential for sustainable energy storage applications. In conclusion, the versatile morphology, environmental compatibility, and structural durability of MgO-based materials make them highly attractive for use in supercapacitors.

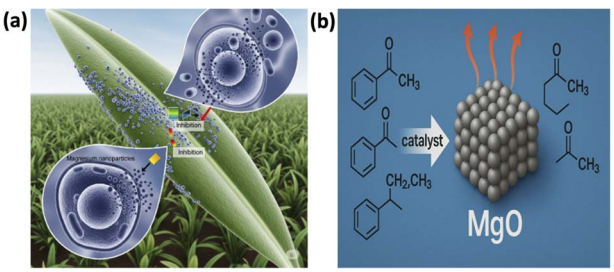

Fig. 13 Illustrates the antibacterial properties of MgO nanoparticles (a) and the catalytic role of MgO (b) in the dehydrogenation of secondary alcohols to ketones.

Electrochemical research is crucial when analyzing the properties and behavior of nanomaterials. Nanomaterials offer unique electrochemical properties due to their enormous surface area, quantum size effects, and enhanced charge transfer kinetics. The performance, stability, reactivity, and electrochemical behavior of nanomaterials can all be better understood using electrochemical techniques. Cyclic voltammetry (CV) and electron impedance spectroscopy (EIS) are two electrochemical techniques that are commonly used to analyze and optimize nanomaterials for a range of applications. CV is a widely used technique to investigate the redox behavior and electrochemical stability of nanomaterials. It provides information about the charge storage capacity, redox potentials, and surface reactions of nanomaterials. EIS is a useful technique for assessing the electrical response of prepared materials and figuring out the charge transfer resistance. Fig. 14 CV plots of MgO made using gel extracts from *Syzygium cumini* (MgO-J) (a), *Citrullus lanatus* (MgO-W) (b), aloe vera (MgO-A) (c), as fuels at different scan rates and EIS spectra (d).[97]

The generated material was examined *via* CV studies for a variety of applications, including super capacitors and batteries. The capacity is mostly caused by pseudo capacitance, and the CV profile of MgO electrodes revealed two oxidation and reduction peaks that show the red-ox mechanism. Peak movements towards the positive and negative potential sides upon increasing the scan rates verified that the constructed electrode was pseudo-capacitive.[178] Electrochemical impedance studies (EIS) were also investigated is represented in Fig. 15(a) CGD, Fig. 15(b) specific capacitance and current, Fig. 15(c) cyclic performance in order to determine the charge transfer resistance and the observed spectra of generated electrodes. It shows an elevated arc (semicircle), and an arc with a larger radius usually indicates a higher charge transfer resistance.[179] MgO-J has a relatively low charge transfer resistance due to its small semicircle radius when compared to other produced electrodes. Furthermore, compared to the other electrodes, the MgO-J electrode exhibits greater capacitive properties.

Recent studies of MgO NPs show that co-precipitation and other state-of-the-art methods exhibit aggregated, porous morphologies that facilitate ion transport and provide readily accessible electrolyte diffusion channels in supercapacitor devices. Computational studies using density functional theory (DFT) support these findings by confirming the structural and electrochemical integrity of MgO nanoparticles through the demonstration of a low HOMO–LUMO energy gap and favourable electronic properties that enable efficient charge transfer and high reactivity.[126] The performance of MgO-based supercapacitors can be significantly enhanced by doping with transition metals, such as vanadium, which introduces extrinsic defects and paramagnetic centres, thereby increasing capacitance and energy density. MgO electrodes doped with vanadium, for example, have demonstrated specific capacitance values up to 50 F g^{-1}. The capacitance values can increase to 1200 F g^{-1} when combined with carbon black or other booster materials, which is much greater than that of pure MgO. Ternary composites of MgO further demonstrate the potential of hybrid MgO nanostructures for high-performance

supercapacitor applications with polyaniline (PANI) and boron nitride nanotubes (BNNTs), which have achieved specific capacitance values exceeding 2000 F g^{-1} and energy densities above 40 Wh kg^{-1} with excellent capacitance retention over multiple cycles.[180] In addition to their electrochemical capabilities, MgO-based materials have benefits for industrial energy storage solutions in terms of affordability, environmental friendliness, and scalability. Their sustainability profile is further improved by their capacity to be synthesized using environmentally friendly techniques, such as those mediated by plant extracts. Optimizing synthesis parameters, investigating novel dopants and composite topologies, and incorporating MgO electrodes into flexible and solid-state supercapacitor devices are the main areas of ongoing study. These developments establish magnesium oxide nanoparticles as a viable basis for high-capacitance, environmentally benign, and next-generation supercapacitor technologies.[180]

5 Challenges and future prospects

Characterization, stability, toxicity, and reproducibility are the main obstacles to the environmentally friendly synthesis of MgO NPs. The manufacture of MgO NPs using green procedures often relies on natural extracts, which vary in composition and effectiveness. The size, shape, and other characteristics of the generated nanoparticles vary widely, making it difficult to compare data with any degree of accuracy. The majority of this green synthesis is carried out on a small scale, which is impractical for large-scale production; for them, developing scaled green production techniques is extremely difficult. MgO NPs produced traditionally might be less stable and more likely to break down and aggregate over time, and increasing the stability of nanoparticles is mandatory. For that, it can be tough to exactly determine the size, shape, and other characteristics of green-synthesized MgO NPs due to their complex and diverse morphologies. The malignancy and biocompatibility of these NPs must also be MgO NPs produced conventionally might be less stable and more likely to break down and aggregate over time. Developing strategies to enhance the stability of nanoparticles is essential. Moreover, it can be challenging to exactly determine the size, shape, and other characteristics of green-synthesized MgO nanoparticles due to their complex and diverse morphologies. The toxicity and biocompatibility of these nanoparticles must also be thoroughly evaluated. Additional research is required to fully understand the potential impacts of MgO NPs produced through green synthesis. Despite the challenges encountered so far, the green synthesis of MgO NPS holds promise for the next generation. The green synthesis of MgO NPs offers several advantages over common methods. MgO NPs have potential applications in biology, medicine, energy storage, batteries, pollution control, catalysis, and various other fields. Their catalytic performance in numerous chemical reactions has been demonstrated in the areas of organic synthesis and environmental catalysis. They can be employed in environmental remediation, green chemistry, and heterogeneous catalysis for organic transformations. Also, these NPs show potential in drug delivery, medical imaging, tissue engineering, and cancer therapy. MgO NPs have also demonstrated strong adsorption capacity for organic pollutants and heavy metals. In the future, it may find applications in air purification, water treatment, and soil remediation, and they could be utilized in agriculture to enhance plant growth and soil fertility. Their use as pesticides and fertilizers holds the potential to promote sustainable farming practices and reduce the reliance on harmful chemical agents. Additionally, research has been done on the application of MgO NPs in energy storage devices such as batteries and supercapacitors. They have the potential to be high-performing and environmentally friendly. Though further research is necessary to realize their potential in these fields fully, MgO nanoparticles have a bright future in a number of applications evaluated. Additional research is required to fully understand the potential impacts of MgO nanoparticles produced through green synthesis. Despite the challenges encountered so

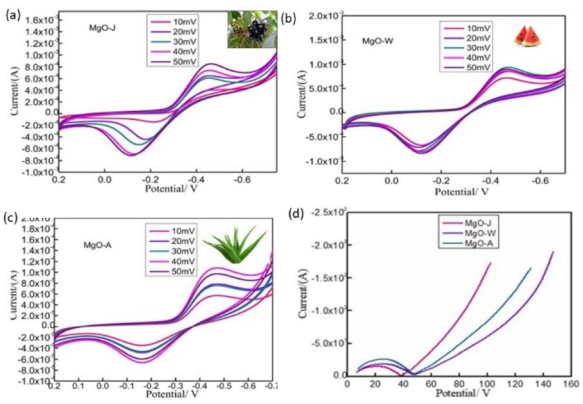

Fig. 14 CV plots of MgO made using extracts from (a) *Syzygium cumini* (MgO-J), (b) *Citrullus lanatus* (MgO-W) gel extracts from (c) aloe vera (MgO-A) at different scan rates and EIS spectra (d).[97] Reproduced from ref. 97, originally published in *NEXT Materials*, Elsevier, under the terms of the CC BY License.

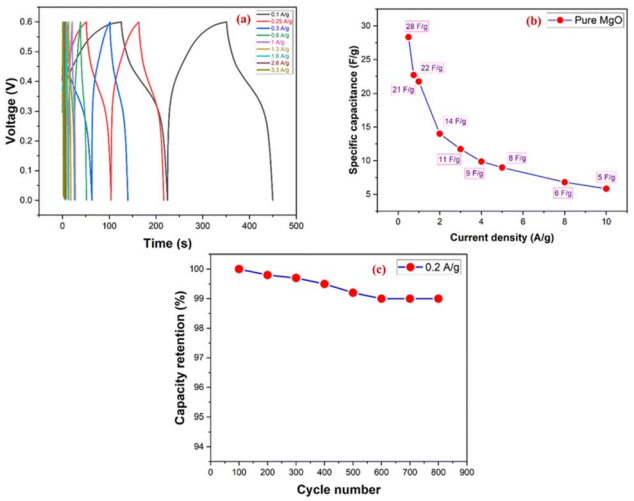

Fig. 15 (a) Different current density of GCD for MgONPs electrodes, (b) the variation of specific capacitance with various current densities of MgONPs electrodes, (c) cyclic performance at 0.2 A g^{-1} (800 cycles) with capacity retention.[176] Reproduced from ref. 176, originally published in *RSC Advances*, RSC, under the terms of the CC BY License.

far, the green synthesis of MgO nanoparticles holds great promise for the future. The green synthesis of magnesium oxide nanoparticles offers several advantages over traditional methods commonly used. MgO nanoparticles have potential applications in biology, medicine, energy storage, batteries, pollution control, catalysis, and various other fields. Their catalytic performance in numerous chemical reactions has been demonstrated in the areas of organic synthesis and environmental catalysis. They can be employed in environmental remediation, green chemistry, and heterogeneous catalysis for organic transformations. Moreover, these nanoparticles show potential in drug delivery, medical imaging, tissue engineering, and cancer therapy. MgO nanoparticles have also demonstrated strong adsorption capacity for organic pollutants and heavy metals. In the future, MgO nanoparticles may find applications in air purification, water treatment, and soil remediation. Additionally, they could be utilized in agriculture to enhance plant growth and soil fertility. Their use as pesticides and fertilizers holds the potential to promote sustainable farming practices and reduce the reliance on harmful chemical agents. The research has been done on the application of MgO NPs in energy storage devices such as batteries and supercapacitors. They have the potential to be high-performing and environmentally friendly. Though further research is necessary to realize their potential in these fields fully, MgO nanoparticles have a bright future in a number of applications.

MgO nanoparticles can be processed onto textile fabrics using various techniques, and the padding method is among the most common at both the lab and industrial levels. This process involves treating the fabric with a solution containing MgO nanoparticles then rolling the fabric to ensure that it has a uniform coating. The applied chemicals in the fabric are then allowed to dry and cure, completing the application. It has been reported recently that, using the pad-dry-cure method, MgO nanoparticles were incorporated into the cotton fabric. Before applying the synthesized nanoparticles, they were dispersed in de-ionized water using a mechanical stirrer. In the current study, a 100% cotton fabric sample was treated with 2% MgO nanoparticles and 3% citric aciviang fabric-soakingng process. Another benefit of the padding method is that wet pickup cannot be compromised, and the coating solution is uniformly distributed on the fabric.[181] Numerous techniques have been adopted to apply the nanoparticles to the fabric surface. Dip coating includes the step in which the fabric is immersed in a nanoparticle suspension, soaked for a set duration, and then withdrawn at a controlled speed. The advantage of the full-pickup technique the (without squeezing). The films are developed without employing any capping agent and catalyst. A simple chemical deposition technique is adopted for this purpose.[182] Another method for covering the uneven surface with a more uniform coating of particles is spraying. MgO nanoparticles were sprayed onto the textile surface after being dispersed in a solvent in a recent study. Even dispersion is made possible by the method, which works especially well for coating uneven surfaces. The method provides controlled deposition and is applicable to a variety of coatings. The chemical solution immersion method, which results in the sol–gel technique, is an additional substitute for mechanical deposition. Methyl trimethyl silane (MTMS) (6 ml) and non-ionic polyethylene glycol (PEG) surfactant (2 ml) were combined to create the silica hydrosol 180 ml of 100% ethanol was then mixed with 6 ml of deionized water and rapidly agitated for 15 minutes at room temperature to create a homogenous solution. 4 ml of ammonia was then gradually added to this solution while being constantly stirred. After that, the methyl silicate sol was vigorously stirred for 15 minutes at room temperature while MgO nanoparticles (1 g) were added. A MgO/methyl silicate composite sol was then formed by subjecting the solution to ultrasonic irradiation for 30 minutes.[183]

Several approaches can be used to overcome the present constraints and fully utilize green-synthesised MgO NPs. By standardizing extraction and reaction parameters, it is possible to reduce batch-to-batch variations and achieve more consistent particle properties during synthesis. Accurately determining the size, shape, and composition of nanoparticles requires advanced characterization techniques such as high-resolution electron microscopy and various spectroscopic methods, especially when working with complex green extracts. To achieve industrial-scale production while maintaining cost-effectiveness and environmental sustainability, improvements in reactor design and process scaling are essential. In addition, the use of high-throughput screening methods can speed up biological evaluations and the optimization of synthesis conditions. Collaborative efforts among biologists, engineers, and chemists can further drive the development of innovative green synthesis methods and promote sustainable applications. As nanoscale regulatory frameworks evolve, stricter safety, toxicological, and environmental requirements will ensure the proper use of MgO NPs in a range of industries.

6 Conclusions

In recent years, green synthesis of metal oxide nanoparticles has gained prominence due to environmental concerns associated with traditional physical and chemical methods. Out of various metal oxides, MgO has emerged as a potentially suitable candidate due to its exceptional physicochemical properties, stability, biocompatibility, and large surface area. These characteristics make MgO an ideal material for environmental remediation, wastewater treatment, and antibacterial applications. This comprehensive review synthesizes insights from both conventional and green synthesis strategies, contributing to the sustainable development of nanotechnology. Among the green synthesis methods discussed, the production of MgO nanoparticles using plant extracts is a promising approach. This method offers the potential to produce nanoparticles with controlled size, low toxicity, enhanced surface interactions, and reproducibility, all while minimizing the production of hazardous by-products.

Author contributions

G. Georgelin Jeba Mahiba: writing – review & editing, writing – original draft, data curation, conceptualization. A. Prabakaran: supervision, resources, software, methodology, investigation.

Babu Balraj: validation, formal analysis, resources, methodology. All the authors read and approved the final version of the manuscript.

Conflicts of interest

The authors declare that they have no known competing financial interests or personal relationships that could have influenced the work reported in this paper.

Abbreviations

SP	Sol-precipitation
CC	Chemical combustion NPs-nano particles
CV	Cyclic voltammetry
EIS	Electro chemical impedance spectra
GM	Green method
MgO	Magnesium oxide
HEBM	High energy ball milling
FSP	Flame spray pyrolysis
CTAB	Cetyl trimethyl ammonium bromide
NaOH	Sodium hydroxide
HTM	Hydro thermal method
SEM	Scanning electron microscope
CCS	Carbon capture and storage
CO	Carbon monoxide
TDS	Total dissolved solids
TSS	Total suspended solids
CNT	Carbon nanotubes
MRSA	Methicillin-resistant *Staphylococcus aureus*
PAO1	Polyphosphate-sccumulating organisms
UPF	Microbial enumeration tests
PVDF	Poly vinyl dene fluoride
ROS	Reactive oxygen species
OCM	Oxidative coupling of methane
MTMS	Methyl tri methoxy silane
PEG	Poly ethylene glycol
VAFs	Virulence associated factors
MWC	Microwaves combustion
rGO	reduced graphene oxide
PPY	Poly pyrrole

Data availability

This review article does not contain any new primary data. The data supporting this study are derived from previously published articles, which have been cited appropriately. Any compiled data presented in tables or figures are based on information available in the referenced literature.

Acknowledgements

One of the authors, A. Prabakaran would like to thank the financial support from Vel Tech Rangarajan Dr.Sagunthala R&D Institute of Science and Technology under the Research Development Fund (RDF) FY 2025-26/059. The authors declare that ChatGPT-5.1 (OpenAI) was used solely for language polishing, grammar correction, and enhancing clarity and readability of the manuscript. All scientific content, analysis, interpretations, and conclusions in this study are entirely original and generated by the authors.

References

1 S. Malik, K. Muhammad and Y. Waheed, *Molecules*, 2023, **28**(2), 661.
2 M. Rostami, A. S. Nasab, M. Fasihi-Ramandi, A. Badiei, M. Rahimi-Nasrabadi and F. Ahmadi, *New J. Chem.*, 2021, **45**, 4280–4291.
3 T. A. Saleh, *Environ. Technol. Innov.*, 2020, **20**, 101067.
4 B. D. Malhotra and M. A. Ali, Chapter 1-Nanomaterials in Biosensors: Fundamentals and Applications, in *Nanomaterials for Biosensors*, ed. B. D. Malhotra and M. D. A. Ali, William Andrew Publishing, Norwich, NY, USA, 2018, pp. 1–74.
5 K. Khalid, X. Tan, H. F. Mohd Zaid, Y. Tao, C. L. Chew, D.-T. Chu, M. K. Lam, Y.-C. Ho, J. W. Lim and L. C. Wei, *Bioengineered*, 2020, **11**, 328–355.
6 S. A. M. Ealia and M. P. Saravanakumar, *IOP Conf. Ser. Mater. Sci. Eng.*, 2017, **263**, 032019.
7 A. Cartwright, K. Jackson, C. Morgan, A. Anderson and D. W. Britt, *Agronomy*, 2020, **10**, 1018.
8 K. M. Koczkur, M. Mourdikoudis, S. Polavarapu and L. M. Skrabalak, *Dalton Trans.*, 2015, **44**, 17883–17905.
9 A. A. Yaqoob, H. Ahmad, T. Parveen, A. Ahmad, M. Oves, I. M. I. Ismail, H. A. Qari, K. Umar and M. N. Mohamad Ibrahim, *J. Mol. Liq.*, 2020, **310**, 113279.
10 M. Chinthala, A. Balakrishnan, P. Venkataraman, V. Manaswini Gowtham and R. K. Polagani, *Environ. Chem. Lett.*, 2021, **19**, 4415–4454.
11 H. M. Fahmy, M. H. El Hakim, D. S. Nady, Y. M. Elkaramany, F. A. Mohamed, A. M. Yasien, M. A. Moustafa, B. E. Elmsery and H. A. Yousef, *Nanomed. J.*, 2022, **9**, 1–14.
12 B. Babu, B. Mohanbabu, S. Kumar Nagarajan, M. Raja and M. Balaj, *NanoNEXT*, 2023, **4**, 1–31.
13 M. S. S. Danish, A. Bhattacharya, D. Stepanova, A. Mikhaylov, M. L. Grilli, M. Khosravy and T. Senjyu, *Metals*, 2020, **10**, 1604.
14 M. S. Chavali and M. P. Nikolova, *SN Appl. Sci.*, 2019, **1**, 607.
15 P. P. Kumar, M. L. D. Bhatlu, K. Sukanya, S. Karthikeyan and N. Jayan, *Mater. Today Proc.*, 2021, **37**, 3028–3030.
16 M. Hajibeygi, M. Mousavi, M. Shabanian, N. Habibnejad and H. Vahabi, *Mater. Chem. Phys.*, 2021, **258**, 123917.
17 R. Narayanan and M. A. Sakthivel, *Adv. Colloid Interface Sci.*, 2010, **156**, 1–13.
18 A. R. Biris, E. Dervishi, S. Ardelean, M. D. Lazar, F. Watanabe, G. L. Biris and A. S. Biris, *Mater. Chem. Phys.*, 2013, **138**, 454–461.
19 S. Kaabipour and S. Hemmati, *Beilstein J. Nanotechnol.*, 2021, **12**, 102–136.
20 T. Duffy, N. Madhusudhan and K. K. M. Lee, 2.07-Mineralogy of Super-Earth Planets, in *Treatise on*

Geophysics, ed. G. Schubert, Elsevier, Oxford, UK, 2nd edn, 2015, pp. 149–178.
21 A. D. Akinwekomi, C.-Y. Tang, G. C.-P. Tsui, W.-C. Law, L. Chen, X.-S. Yang and M. Hamdi, *Mater. Des.*, 2018, **160**, 591–600.
22 J. P. Singh and K. H. Chae, *Condens. Matter*, 2017, **2**, 4.
23 J. Hornak, *Int. J. Mol. Sci.*, 2021, **22**, 12752.
24 K. Ramanujam and M. Sundrarajan, *J. Photochem. Photobiol., B*, 2014, **141**, 296–300.
25 W. A. Ali, S. E. Richards and R. H. Alzard, *J. Ind. Eng. Chem.*, 2025, **149**, 63–93.
26 T. Xing, J. Sunarso, W. Yang, Y. Yin, A. M. Glushenkov, L. H. Li and Y. Chen, *Nanoscale*, 2013, **5**, 7970–7976.
27 S. Rashid, S. Islam, S. Qamer, M. Ali, M. Fatima, L. Javaid, A. Ali, A. Sarwar, A. S. Farooq, M. Waqas, B. Khalid, N. S. Awwad, H. A. Ibrahium and M. A. Bajaber, *J. Ind. Text.*, 2025, **55**, https://10.1177/15280837251313518.
28 N. T. T. Nguyen, L. M. Nguyen, T. T. T. Nguyen, U. P. N. Tran, D. T. C. Nguyen and T. Van Tran, *Chemosphere*, 2023, **312**, 137301.
29 R. B. Rotti, D. V. Sunitha, R. Manjunath, A. Roy, S. Borehalli Mayegowda, A. P. Gnanaprakash, S. Alghamdi, M. Almehmadi, O. Abdulaziz, M. Allahyani, A. Aljuaid, A. Amer Alsaiari, S. S. Ashgar, A. O. Babalghith, A. Ezzat Abd El-Lateef and E. B. Khidir, *Front. Chem.*, 2023, **11**, 1143614.
30 S. Abinaya, H. P. Kavitha, M. Prakash and A. Muthukrishnaraj, *Sustainable Chem. Pharm.*, 2023, **19**, 100368.
31 A. Purwanto, W. N. Wang and K. Okuyama, Flame spray pyrolysis, in *Handbook of Atomization and Sprays: Theory and Applications*, Springer US, Boston, MA, USA, 2010, pp. 869–879.
32 N. Ashgriz, *Handbook of Atomization and Sprays: Theory and Applications*, Springer Science & Business Media, 2011.
33 V.-I. Merupo, S. Velumani, K. Ordon, N. Errien, J. Szade and A.-H. Kassiba, *RSC Adv.*, 2016, **6**, 53466–53474.
34 W. Y. Teoh, R. Amal and L. Mädler, *Nanoscale*, 2010, **2**, 1324–1347.
35 M. T. Mhetre, H. M. Pathan, A. V. Thakur and B. J. Lokhande, *ES Energy Environ.*, 2022, **18**, 41–46.
36 R. Wallace, A. P. Brown, R. Brydson, K. Wegner and S. J. Milne, *J. Mater. Sci.*, 2013, **48**, 6393–6403.
37 A. I. Y. Tok, F. Y. C. Boey and X. L. Zhao, *J. Mater. Process. Technol.*, 2006, **178**, 270–273.
38 R. Mueller, L. Mädler and S. E. Pratsinis, *Chem. Eng. Sci.*, 2003, **58**, 1969–1976.
39 L. D. Hafshejani, S. Tangsir, H. Koponen, J. Riikonen, T. Karhunen, U. Tapper and A. Lähde, *Powder Technol.*, 2016, **298**, 42–49.
40 Z. U. Abideen, W. U. Arifeen and A. Tricoli, *Nanoscale*, 2024, **16**, 7752–7785.
41 G. A. G. Solero, *Nanosci. Nanotechnol.*, 2017, **7**, 21–25.
42 L. V. Maximiano, L. B. Correa, N. C. Gomes-da-Silva, L. S. da Costa, M. G. P. Da Silva, A. V. Chaves and D. M. A. Neto, *Colloids Surf., B*, 2024, **239**, 113931.
43 A. C. Gurule, S. S. Gaikwad, D. D. Kajale, V. S. Shinde, G. R. Jadhav and V. B. Gaikwad, *J. Indian Chem. Soc.*, 2025, **102**, 101496.
44 S. Bhuvaneshwari, S. Satheeskumar, J. Velayutham and B. S. Rahman, *Rasayan J. Chem.*, 2021, **14**, 1581–1586.
45 Z. Rajabimashhadi, R. Naghizadeh, A. Zolriasatein and C. Esposito Corcione, *Nanomaterials*, 2023, **13**, 454.
46 X. Song, Z. Qiu, X. Yang, H. Gong, S. Zheng, B. Cao, H. Wang, H. Möhwald and D. Shchukin, *Chem. Mater.*, 2014, **26**(17), 5113–5119.
47 Z. Rajabimashhadi, M. Mirzaeei and E. Zulfugar, *Appl. Surf. Sci.*, 2023, **598**, 153799.
48 Z. X. Tang, D. M. W. Leung and W. Liu, *Brazilian J. Chem. Eng.*, 2014, **31**, 555–562.
49 X. Wang, M. Khan, F. Zhang, Y. Zhao, J. Li and W. Xu, *Polymers*, 2021, **13**, 1445.
50 J. Sharma, M. Sharma and S. Basu, *J. Environ. Chem. Eng.*, 2017, **5**, 3429–3438.
51 K. N. Pandian, S. Palanichamy, S. Anbalagan, P. Rajendran, G. K. Poongavanam, S. Kim, A. Alodhayb, P. Saravanan, R. Elansezhian and R. Muraliraja, *Arabian J. Chem.*, 2023, **16**, 105028.
52 K. G. Manjunatha, B. E. Kumara Swamy, H. D. Madhuchandra, K. J. Gururaj and K. A. Vishnumurthy, *Sensors Int.*, 2021, **2**, 100127.
53 X. Song, Z. Qiu, X. Yang, H. Gong, S. Zheng, B. Cao, H. Wang, H. Möhwald and D. Shchukin, *ACS Appl. Mater. Interfaces*, 2014, **6**, 5981–5987.
54 W. Gao, T. Zhou, B. Louis and Q. Wang, *Catalysts*, 2017, **7**(4), 116.
55 P. Bhattacharya, S. Swain, L. Girib and S. Neogi, *J. Mater. Chem. B*, 2019, **7**, 4141–4152.
56 S. Shijina, Sainudeen, L. B. Asok, A. Varghese, A. Sreekumaran Naira and G. Krishnan, *RSC Adv.*, 2017, **7**, 35160–35168.
57 C. J. Brinker and G. W. Scherer, *Sol–Gel Science: The Physics and Chemistry of Sol–Gel Processing*, Academic Press, San Diego, 1990.
58 J. Hornak, *Int. J. Mol. Sci.*, 2021, **22**, 12704.
59 B. Vatsha, P. Tetyana, P. Shumbula, J. Ngila, L. Sikhwivhilu and R. Moutloali, *J. Biomater. Nanobiotechnol.*, 2013, **4**, 365–373.
60 T. Adschiri, K. Kanazawa and K. Arai, *Ind. Eng. Chem. Res.*, 2000, **39**, 4901–4907.
61 D. Navas, S. Fuentes, A. Castro-Alvarez and E. Chavez-Angel, *Gels*, 2021, **7**, 275.
62 R. Yarbrough, K. Davis, S. Dawood and H. Rathnayake, *RSC Adv.*, 2020, **10**, 14134–14146.
63 S. M. Abegunde, B. O. Afolayan and T. M. Ilesanmi, *Sustainable Chemistry One World*, 2024, **3**, 100014.
64 H. Singh, M. F. Desimone, S. Pandya, S. Jasani, N. George, M. Adnan, A. Aldarhami, A. S. Bazaid and S. A. Alderhami, *Int. J. Nanomed.*, 2023, **18**, 4727–4750.
65 A. Varma, A. S. Mukasyan, A. S. Rogachev and K. V. Manukyan, *Chem. Rev.*, 2016, **116**, 14493–14586.
66 D. Gupta, A. Boora, A. Thakur and T. K. Gupta, *Environ. Res.*, 2023, **231**, 116316.

67 D. Kumar, L. S. Reddy Yadav, K. Lingaraju, K. Manjunath, D. Suresh, D. Prasad, H. Nagabhushana, S. C. Sharma, H. Raja Naika, Chikkahanumantharayappa and G. Nagaraju, *AIP Conf. Proc.*, 2015, **1665**, 050145.
68 S. Aron Rabi, A. T. Ravichandran and A. Joseph Sagaya Kennedy, *Indian J. Nat. Sci.*, 2025, **16**(89), 91651–91655.
69 S. Krishna Moorthy, C. H. Ashok, K. Venkateswara Rao and C. Viswanathan, *Mater. Today Proc.*, 2015, **2**(9), 4360–4368.
70 S. Kiran, H. B. Albargi, G. Afzal, U. Aimun, M. Naveed Anjum, M. Bilal Qadir, Z. Khaliq, M. Jalalah, M. Irfan and M. M. Abdullah, *Appl. Water Sci.*, 2023, **13**, 193.
71 T. R. Rahman, S. Ara, M. I. Hossain, M. T. Islam, T. S. Rahman, H. Khatun and J. Saudi, *Med. Pharm. Sci.*, 2021, **7**(8), 348–357.
72 S. Ali, K. G. Sudha, N. Thirumalaivasan, M. Ahamed, S. Pandiaraj, V. D. Rajeswari, Y. Vinayagam, M. Thiruvengadam and R. Govindasamy, *Bioengineering*, 2023, **10**, 302.
73 M. I. Khan, M. N. Akhtar, N. Ashraf, J. Najeeb, H. Munir, T. I. Awan, M. B. Tahir and M. R. Kabli, *Appl. Nanosci.*, 2020, **10**, 2351–2364.
74 T. R. Ananda, S. Archana, L. S. Reddy Yadav, B. M. Shilpa, G. Nagaraju and B. K. Jayanna, *Mater. Today Proc.*, 2022, **49**, 801–810.
75 S. Ashok Kumar, M. Jarvin, S. Sharma, A. Umar, S. S. R. Inbanathan and A. K. Nayak, *ES Food Agrofor.*, 2021, **5**, 14–19.
76 D. Gingaşu, I. Mîndru, D. C. Culiță, L. Predoană, G. Petcu, E. M. Ciobanu, S. Preda, J. Pandele-Cuşu and S. Petrescu, *Rev. Roum. Chim.*, 2021, **66**(5), 463–473.
77 M. Abdul, E. A. M. Hamza, K. Hkiri, A. Safdar, S. Azizi and M. Maaza, *Sci. Rep.*, 2024, **14**, 20135.
78 J. Pachiyappan, N. Gnanansundaram, S. Sivamani, N. P. B. P. Sankari, N. Senthilnathan and G. A. Kerga, *J. Nanomater.*, 2022, 6484573.
79 S. Kiran, A. Ashraf, M. Rahmat, G. Afzal, S. Abrar and S. Asif, *Glob. Nest J.*, 2022, **24**(2), 291–296.
80 R. Munir, K. Ali, S. Abbas Zilqurnain Naqvi, M. A. Maqsood, M. Z. Bashir and S. Noreen, *Sep. Purif. Technol.*, 2023, **306**, 122527.
81 D. T. C. Nguyen, H. H. Dang, D.-V. N. Vo, L. G. Bach, T. D. Nguyen and T. Van Tran, *J. Hazard. Mater.*, 2021, **404**, 124146.
82 R. P. Pugazhendhi, K. Muruganantham, R. Shanmuganathan and S. Natarajan, *J. Photochem. Photobiol., B*, 2019, **190**, 86–97.
83 A. FoudaS, E. D. Hassan, E. Saied and M. F. Hamza, *J. Environ. Chem. Eng.*, 2021, **9**, 105346.
84 M. Ramezani Farani, M. Farsadrooh, I. Zare, A. Gholami and O. Akhavan, *Catalysts*, 2023, **13**(4), 642.
85 M. K. Y. Soliman, A. Hussain Talib, R. Mahmoud, Z. A. Ali, H. H. Al-Haideri, A. Abalkhail, A. S. Binshaya, M. H. Salem, F. O. Al-Otibi and M. Taha Yassin, *AMB Express*, 2025, **15**, 143.
86 D.-M. Radulescu, I. Andreea Neacsu, B. Stefan Vasile, V.-A. Surdu, O.-C. Oprea, R.-D. Trusca, C. Chircov, R. Cristina Popescu, C.-I. Ilie and E. Andronescu, *Int. J. Mol. Sci.*, 2025, **26**(18), 9021.
87 D. Eissa, R. H. Hegab, A. Abou-Shady and Y. H. Kotp, *Sci. Rep.*, 2022, **12**, 5780.
88 K. Jashvant Kumar, J. Daimari, S. Basumatary, A. Mondal and A. Kalita Deka, *Sci. Rep.*, 2025, **15**, 21749.
89 N. M. Al Musayeib, M. Amina, F. Maqsood, K. A. Bokhary and N. S. Alrashidi, *Bioinorg. Chem. Appl.*, 2024, **2024**, 8180102.
90 S. P. Patil, R. Y. Chaudhari and M. S. Nemade, *Talanta Open*, 2022, **5**, 100083.
91 S. Mushtaq, Z. Yousaf, I. Anjum, S. Arshad, A. Aftab, Z. Maqbool, Z. Shahzadi, R. Ullah and E. A. Ali, *Food Chem. X*, 2024, **21**, 101157.
92 K. Jhansi, N. Jayarambabu, K. P. Reddy, N. M. Reddy, R. P. Suvarna, K. V. Rao, V. R. Kumar and V. Rajendar, *3 Biotech*, 2017, **7**, 263.
93 T. Elsakhawy, A. E.-D. Omara, M. Abowaly, H. El-Ramady, K. Badgar, X. Llanaj, G. Törős, P. Hajdú and J. Prokisch, *Sustainability*, 2022, **14**, 4328.
94 R. Supreetha, S. Bindya, P. Deepika, H. M. Vinusha and B. P. Hema, *Results Chem.*, 2021, **3**, 100156.
95 A. Farina Farizan, H. M. Yusoff, N. Badar, I. Ul Haq Bhat, S. Jaheera Anwar, C. Poh Wai, A. Asari, M. F. Kasim and K. Elong, *Arabian J. Sci. Eng.*, 2022, **48**, 7373–7386.
96 E. R. Essien, V. N. Atasie, A. O. Okeafor and D. O. Nwude, *Int. Nano Lett.*, 2020, **10**, 43–48.
97 L. Ramakrishna, R. Thippeswamy, G. K. Mallesh and S. K. Kempahanumakkagari, *Next Mater.*, 2024, **4**, 100193.
98 A. Kumar and J. Kumar, *J. Phys. Chem. Solids*, 2008, **69**, 2764–2772.
99 M. R. Mohammad Shafiee, M. Kargar and M. Ghashang, *Green Process. Synth.*, 2018, **7**, 248–254.
100 M. Shkir, T. H. AlAbdulaal, M. Aslam Manthrammel and F. S. Khan, *J. Photochem. Photobiol., A*, 2024, **449**, 115398.
101 W. B. Ayinde, M. W. Gitari, M. Muchindu and A. Samie, *J. Nanotechnol.*, 2018, **2018**, 9537454.
102 M. W. Alam, *Appl. Organomet. Chem.*, 2025, **39**, e7899.
103 H. Bhoi, S. Tiwari, Manisha, V. K. Salvi, P. Seal, S. K. Modi, G. Lal, P. L. Mange, V. Saharan, J. P. Borah, S. K. Barbar, K. B. Modi and S. Kumar, *Mater. Chem. Phys.*, 2025, **346**, 131332.
104 T. Jeena, M. P. Geetha, P. A. Suchetan, N. Ronald and K. Amrutha, *Inorg. Chem. Commun.*, 2023, **157**, 111232.
105 D. Chauhan, R. Kumar, N. Thakur, M. Singh and K. Kumar, *Hybrid Adv.*, 2024, **6**, 100199.
106 S. Ying, Z. Guan, P. C. Ofoegbu, P. Clubb, C. Rico, F. He and J. Hong, *Environ. Technol. Innov.*, 2022, **26**, 102336.
107 Z. Villagrán, L. M. Anaya-Esparza, C. A. Velázquez-Carriles, J. M. Silva-Jara, J. M. Ruvalcaba-Gómez, E. F. Aurora-Vigo, E. Rodríguez-Lafitte, N. Rodríguez-Barajas, I. Balderas-León and F. Martínez-Esquivias, *Resources*, 2024, **13**(6), 70.
108 N. Ahmed, B. Zhang, B. Bozdar, S. Chachar, M. Rai, J. Li, Y. Li, F. Hayat, Z. Chachar and P. Tu, *Front. Plant Sci.*, 2023, **14**, 1285512.
109 M. Lavanya and S. Karthick Raja Namasivayam, *Plant Nano Biol.*, 2025, **14**, 100200.

110 A. M. Nelwamondo, A. G. Kaningini, T. Y.-a. Ngmenzuma, S. T. Maseko, M. Maaza and K. C. Mohale, *Heliyon*, 2023, **9**(9), e19419.
111 A. M. Nelwamondo, M. Maaza and K. C. Mohale, *Biocatal. Agric. Biotechnol.*, 2024, **59**, 103246.
112 Z. Abbas, M. A. Hassan, W. Huang, H. Yu, M. Xu, X. Chang and L. Liu, *Agronomy*, 2024, **14**, 617.
113 A. Jha, D. Pathania, Sonu, B. Damathia, P. Raizada, S. Rustagi, P. Singh, G. M. Rani and V. Chaudhary, *Environ. Res.*, 2023, **235**, 116456.
114 L. Cai, J. Chen, Z. Liu, H. Wang, H. Yang and W. Ding, *Front. Microbiol.*, 2018, **9**, 790.
115 N. Sharma, B. Allardyce, R. Rajkhowa, A. Adholeya and R. Agrawal, *Front. Plant Sci.*, 2022, **13**, 895740.
116 C. Xiong, W. Wang, F. Tan, F. Luo, J. Chen and X. Qiao, *J. Hazard. Mater.*, 2015, **299**, 664–674.
117 S. Faisal, S. Naqvi, M. Ali and L. Lin, *Pigment Resin Technol.*, 2022, **51**, 301–308.
118 J. Liao, Z. Yuan, X. Wang, T. Chen, K. Qian, Y. Cui, A. Rong, C. Zheng, Y. Liu, D. Wang and L. Pan, *Front. Microbiol.*, 2024, **15**, 1370427.
119 S. Ali, Z. Ulhassan, H. Shahbaz, Z. Kaleem, M. A. Yousaf, S. Ali, M. S. Sheteiwy, M. Waseem, S. Ali and W. Zhou, *Environ. Sci.: Nano*, 2024, **11**, 3250–3267.
120 A. Ohadian, N. Khayat, M. Mokhberi and S. Horpibulsuk, *Transp. Geotech.*, 2024, **46**, 101261.
121 S. Chen, P. Ni, Z. Sun and K. Yuan, *Sustainability*, 2023, **15**, 4344.
122 M. El Sharkawy, A. A. AL Huqail, A. M. Aljuaid, N. Kamal, E. Mahmoud, A. E. Omara, N. A. El Kader, J. Li, N. N. Mahmoud, A. A. El Baroudy and S. M. Ismail, *Nanomaterials*, 2024, **14**, 1164.
123 K. Lavanya, B. Kanthimathi and J. Sundararajan, *Plant Nano*, 2025, **5**, 100200.
124 A. Junior Ogliari, W. G. Borges, L. Luiz Silva, J. M. M. de Mello, D. Baretta, M. . Antônio Fiori and C. R. D. M. Barett, *J. Appl. Toxicol.*, 2022, **42**, 553–569.
125 G. B. Pour, M. K. Oroumiyeh and L. F. Aval, *Case Stud. Chem. Environ. Eng.*, 2025, **11**, 101042.
126 S. Zhao and J. Zou, *Powder Technol.*, 2021, **377**, 506–513.
127 X. Zhao, J. Li, Z. Yang, D. Li, Z. Liu, R. Zhu, C. Wang, C. Zhou, K. Ma, L. Song and H. Yue, *Chem. Eng. Sci.*, 2025, **306**, 121148.
128 N. T. Thao Nguyen, L. Minh Nguyen, T. T. Thanh Nguyen, U. P. N. Tran, D. T. Cam Nguyen and T. Van Tran, *Chemosphere*, 2023, **312**, 137301.
129 T. H. Y. Duong, T. Nhan Nguyen, T. O. Ho, A. D. T. Tuyet, N. T. G. Le, T. P. Hoang, T. A. Nguyen, Ba M. Nguyen, V. Tran Quang, G. Truong Le and T. Van Nguyen, *Vietnam J. Chem.*, 2019, (1), 4376429.
130 S. E.-D. Hassan, A. Fouda, E. Saied, M. M. S. Farag, A. M. Eid, M. G. Barghoth, M. A. Awad, M. F. Hamza and M. F. Awad, *J. Fungi*, 2021, 7(5), 372.
131 E. Saied, A. M. Eid, S. E.-D. Hassan, S. S. Salem, A. A. Radwan, M. Halawa, F. M. Saleh, H. A. Saad, E. M. Saied and A. Fouda, *Catalysts*, 2021, **11**(7), 821.
132 H. Ruhaimi, M. A. A. Aziz and A. A. Jalil, *J. CO_2 Util.*, 2021, **43**, 101357.
133 H. C. S. Pereraa, V. Gurunanthanan, A. Singh, M. M. M. G. P. G. Mantilaka, G. Das and S. Arya, *J. Magnesium Alloys*, 2024, **12**(5), 1709–1773.
134 J. Fawell, K. Bailey, J. Chilton, E. Dahi, L. Fewtrell and Y. Magara, *Fluoride in Drinking-Water*, World Health Organization (WHO), Printed by TJ International (Ltd), Padstow, Cornwall, UK, 2006.
135 S. Ahmad, R. Singh, T. Arfin and K. Neeti, *Environ. Sci.:Adv.*, 2022, **1**, 620–661.
136 V. Mariappan Santhi, D. Periasamy, M. Perumal, P. M. Sekar, V. Varatharajan, D. Aravind, K. Senthilkumar, S. T. Kumaran, S. Ali, S. Sankar, N. Vijayakumar, C. Boominathan and R. S. Krishnan, *Sustainability*, 2024, **16**(24), 11056.
137 P. Pillai, S. Dharaskar, S. Pandian and H. Panchal, *Environ. Technol. Innov.*, 2021, **21**, 101246.
138 M. Habuda-Stanić, M. Ergović Ravančić and A. Flanagan, *Materials*, 2014, **7**, 6317–6366.
139 S. L. M. Rubright, L. L. Pearce and J. Peterson, *Nitric Oxide*, 2017, **71**, 1–13.
140 J. A. Rodriguez, T. Jirsak and S. Chaturvedi, *J. Chem. Phys.*, 1999, **111**, 8077–8087.
141 I. W. Siriwardane, R. Udangawa, R. M. de Silva, A. R. Kumarasinghe, R. G. Acres, A. Hettiarachchi, G. A. J. Amaratunga and K. M. N. de Silva, *Mater. Des.*, 2017, **136**, 127–136.
142 V. Singh, G. Ahmed, S. Vedika, P. Kumar, S. K. Chaturvedi, S. N. Rai, E. Vamanu and A. Kumar, *Sci. Rep.*, 2024, **14**, 7595.
143 S. Megarajan, K. R. Kanth and V. Anbazhagan, *Spectrochim. Acta, Part A*, 2020, **239**, 118485.
144 A. Jain, S. Wadhawan, V. Kumar and S. K. Mehta, *Chem. Phys. Lett.*, 2018, **706**, 53–61.
145 P. Zeitz Ruckart, R. L. Jones, J. G. Courtney, T. Telfair LeBlanc, W. Jackson, M. P. Karwowski, P.-Y. Cheng, A. Paul, E. R. Svendsen and P. N. Breysse, *Morb. Mortal. Wkly. Rep.*, 2021, **70**, 1509–1512.
146 V. Kumar, P. Sharma, K. K. Sharma, A. Kumari and D. Kumar, *IET Nanobiotechnol.*, 2018, **12**, 241–253.
147 Health and Safety Authority (HSA), *Liquid Petroleum Gas (LPG)*, available at: https://www.hsa.ie/eng/topics/liquid_petroleum_gas_lpg_/, accessed 01 June 2025.
148 X. Yin, J. Zhang, I. S. Zhao, M. L. Mei, Q. Li and C. H. Chu, *Int. J. Nanomed.*, 2020, **15**, 2555–2562.
149 T. C. Dakal, A. Kumar, R. S. Majumdar and V. Yadav, *Front. Microbiol.*, 2016, **7**, 1831.
150 Z.-X. Tang and B.-F. Lv, *Braz. J. Chem. Eng.*, 2014, **31**, 591–601.
151 L. Huang, D.-Q. Li, Y.-J. Lin, M. Wei, D. G. Evans and X. Duan, *J. Inorg. Biochem.*, 2005, **99**, 986–993.
152 J. Sawai, H. Kojima, H. Igarashi, A. Hashimoto, S. Shoji, T. Sawaki, A. Hakoda, E. Kawada, T. Kokugan and M. Shimizu, *World J. Microbiol. Biotechnol.*, 2000, **16**, 187–194.

153 Y. He, S. Ingudam, S. Reed, A. Gehring, T. P. Strobaugh Jr and P. Irwin, *J. Nanobiotechnol.*, 2016, **14**, 54.
154 R. Muñiz Diaz, P. E. Cardoso-Avila, J. A Pérez Tavares, R. Patakfalvi, V. Villa Cruz, H. Pérez Ladrón de Guevara, O. Gutiérrez Coronado, R. I. Arteaga Garibay, Q. E. Saavedra Arroyo, V. F. Marañón-Ruiz and J. Castañeda Contreras, *Nanomaterials*, 2021, **11**(2), 410.
155 K. Krishnamoorthy, G. Manivannan, S.-J. Kim, K. Jeyasubramanian and M. Premanathan, *J. Nanopart. Res.*, 2012, **14**, 1063.
156 M. Rai, A. Yadav and A. Gade, *Biotechnol. Adv.*, 2009, **27**, 76–83.
157 S. V. G. Kumari, K. Pakshirajan and G. Pugazhenthi, *Mater. Chem. Phys.*, 2023, **294**, 127036.
158 S. Makhluf, R. Dror, Y. Nitzan, Y. Abramovich, R. Jelinek and A. Gedanken, *Adv. Funct. Mater.*, 2005, **15**, 1708–1715.
159 K. B. Yazhini, X. Wang, Q. Zhou and B. O. Stevy, *RSC Adv.*, 2021, **11**, 36379–36390.
160 M. A. Shah, B. M. Pirzada, G. Price, A. L. Shibiru and A. Qurashi, *J. Adv. Res.*, 2022, **38**, 55–75.
161 M.-A. Gatou, E. Skylla, P. Dourou, N. Pippa, M. Gazouli, N. Lagopati and E. A. Pavlatou, *Crystals*, 2024, **14**, 215.
162 A. Hussein and O. H. Sabr, *J. Mech. Eng. Res. Dev.*, 2019, **42**, 23–31.
163 Y. H. Leung, A. M. C. Ng, X. Xu, Z. Shen, L. A. Gethings, M. T. Wong, C. M. N. Chan, M. Y. Guo, Y. H. Ng, A. B. Djurišić, P. K. H. Lee, W. K. Chan, L. H. Yu, D. L. Phillips, A. P. Y. Ma and F. C. C. Leung, *Small*, 2014, **10**, 1171–1183.
164 S. O. Ogunyemi, F. Zhang, Y. Abdallah, M. Zhang, Y. Wang, G. Sun, W. Qiu and B. Li, *Artif. Cells, Nanomed., Biotechnol.*, 2019, **47**, 2230–2239.
165 L. Shkodenko, I. Kassirov and E. Koshel, *Microorganisms*, 2020, **8**(10), 1545.
166 B. B. Seghir, M. Hima, F. Moulatti, I. Sahraoui, I. Ben Amor, S. Zeghoud, H. Hemmami, I. Kouadri, A. Ben Amor, M. Messaoudi, S. Ahmed, A. Rebiai and P. Pohl, *Nanomaterials*, 2023, **13**, 2425.
167 C. Xu, D. I. Enache, R. Lloyd, D. W. Knight, J. K. Bartley and G. J. Hutchings, *Catal. Lett.*, 2010, **138**, 1–7.
168 R. Yuan and Y. Shen, *Bioresour. Technol.*, 2019, **293**, 122076.
169 H. Chowdhury, P. Bhanja, N. Salam, A. Bhaumik and S. M. Islam, *Mol. Catal.*, 2018, **450**, 46–54.
170 M.-A. Gatou, N. Bovali, E. Skylla, P. Dourou, N. Pippa, M. Gazouli, N. Lagopati and E. A. Pavlatou, *Molecules*, 2024, **29**, 4299.
171 M. A. Al-Najar, F. A. J. Al-Doghachi, A. A. A. Al-Riyahee and Y. H. Taufiq-Yap, *Catalysts*, 2020, **10**, 750.
172 E. H. Kim, I. Park, S. Kim, J. F. Kim, Y. H. Choi and H. Lee, *Chem. Eng. J.*, 2024, **499**, 155865.
173 N. Vidal, M. Ventura, M. Orfila, F. Martínez and J. A. Melero, *Biomass Bioenergy*, 2025, **199**, 107936.
174 N. Ataei, A. Karbasi and M. Baghdadi, *Fuel*, 2023, **347**, 128434.
175 Y. Geng, W. Xue, J. Ye, R. Zhang, P. Mishra and J. Zhao, *Green Chem.*, 2025, **27**(16), 4165–4176.
176 M. Goyal, S. Kumar Pandey and N. Bhatnagar, *RSC Adv.*, 2025, **15**, 25209–25220.
177 T. G. Mofokeng, M. P. Motloung, O. M. Ama, and S. S. Ray, Electrochemical Characterization of Nanomaterials, in *Engineering Materials*, Springer, 2022, pp. 11–24.
178 K. Ariyoshi, Z. Siroma, A. Mineshige, M. Takeno, T. Fukutsuka, T. Abe and S. Uchida, *Electrochemistry*, 2022, **90**, 102007.
179 A. Hroub, M. H. Aleinawi, M. Stefan, M. Mihet, A. Ciorita, F. Bakan-Misirlioglu, E. Erdem and A. M. Rostas, *J. Alloys Compd.*, 2023, **958**, 170442.
180 M. Sakaray and S. Chakra Chidurala, *Mater. Today Proc.*, 2024, **98**.
181 N. R. Dhineshbabu, P. Manivasakan, A. Karthik and V. Rajendran, *RSC Adv.*, 2014, **4**, 32161–32173.
182 A. Chaudhari, K. K. Rangan, T. S. Sudarshan, S. R. Singh and S. R. Pillai, reduced bacterial attachment on surface modified hydrophobic fabric surface: a possible approach for safety enhanced packaging material, *NSTI–Nanotech 2014*, 2014, **2**, 231–234.
183 OECD, *Guidance on Sample Preparation and Dosimetry for the Safety Testing of Manufactured Nanomaterials: 2025 Edition (OECD Series on the Safety of Manufactured Nanomaterials and Other Advanced Materials)*, OECD Publishing, Paris, 2025.